

Multichannel processes in relativistic Coulomb excitation mediated by a quantized electromagnetic field

B.F. Bayman

*School of Physics and Astronomy, University of Minnesota,
116 Church Street S.E., Minneapolis, MN 55455, U.S.A.*

and

F.Zardi

*Istituto Nazionale di Fisica Nucleare and Dipartimento di Fisica,
Via Marzolo,8 I-35131 Padova,Italy.*

May 23, 2019

Abstract

Studies of the Coulomb excitation of a target by a relativistic projectile usually assume that the mediating electromagnetic field is a classical field. In this paper, we derive a time-dependent effective potential, that can be used to study the time-development of the target wave function, which takes into account the fact that the mediating electromagnetic field is actually quantized. This effective potential is free of the difficulties associated with the classical mediating field, namely the divergence at high bombarding energies of certain excitation cross-sections. The results of some coupled-channel calculations indicate significant differences for bombarding energies per nucleon ≥ 2 GeV, between calculations using the classical or quantized electromagnetic fields.

1 Introduction

What has become the standard approach to relativistic Coulomb excitation (RCE) was proposed by A. Winter and K. Alder (WA) in 1979 [1]. The projectile nucleus is assumed to travel along a straight-line orbit parallel to the \hat{z} axis, with impact parameter \mathbf{b} , at constant speed v . The magnitude of the impact parameter is large enough so that nuclear interactions between the target and projectile are negligible. Because of the assumed large projectile momentum, the electromagnetic impulse the projectile receives due to its interaction with the target has little effect on its trajectory, so the projectile maintains its constant speed and impact parameter throughout the collision. As the projectile passes, the target nucleus feels the time-dependent projectile electromagnetic fields, which induce transitions between the quantum states of the target. Starting from the assumption that the target is in its ground state at $t = -\infty$, WA

used first-order perturbation theory to calculate the occupation probabilities of excited target states at $t = +\infty$, and used these probabilities to obtain Coulomb excitation cross-sections¹.

An important ingredient in the calculation of target transition probabilities is the interaction potential felt by the target as the projectile moves past it. WA took this to be the classical electromagnetic field of the moving projectile. A justification of this assumption can be found in the work of Alder, Bohr, Huus, Mottelson and Winther (ABHMW) [4]. These authors used the lowest-order of perturbation theory to calculate the target transition amplitude as a result of photon exchange with the projectile, in a situation in which the projectile motion was described by quantum mechanics. They found that this photon-induced transition amplitude was the same as the target transition amplitude induced by the classical electromagnetic field of the projectile, again calculated in the lowest order of perturbation theory.

To express the result of ABHMW more precisely, let $V_{\text{cl}}(t)$ be the interaction potential experienced by the target nucleus at time t due to the classical electromagnetic field of the projectile. Similarly, let $V_{\text{eff}}(t)$ be the *effective* interaction potential experienced by the target nucleus at time t as a result of photon exchange with the projectile. Consider two unperturbed target states, ϕ_γ and ϕ_α , and let the matrix elements of $V_{\text{cl}}(t)$ and $V_{\text{eff}}(t)$ between these states be labelled by $[V_{\text{cl}}(t)]_{\gamma\alpha}$ and $[V_{\text{eff}}(t)]_{\gamma\alpha}$. Then the statement that $V_{\text{cl}}(t)$ and $V_{\text{eff}}(t)$ yield the same lowest-order transition amplitude between ϕ_γ and ϕ_α implies that the Fourier transforms of $[V_{\text{cl}}(t)]_{\gamma\alpha}$ and $[V_{\text{eff}}(t)]_{\gamma\alpha}$ are equal, when evaluated at the *onshell* frequency associated with the transition

$$\omega_{\gamma\alpha} \equiv \frac{\epsilon_\gamma - \epsilon_\alpha}{\hbar}. \quad (1.1)$$

This is essentially the result of ABHMW. Of course, this does not mean that $[V_{\text{cl}}(t)]_{\gamma\alpha}$ and $[V_{\text{eff}}(t)]_{\gamma\alpha}$ are identical functions of t : the only property that these functions share is their Fourier component evaluated at the frequency (1.1). But this is sufficient to guarantee that first-order perturbation calculations done with $V_{\text{cl}}(t)$ and $V_{\text{eff}}(t)$ will yield the same results. Since WA used first-order perturbation theory in their treatment of RCE, they were able to use $V_{\text{cl}}(t)$ instead of the more fundamental $V_{\text{eff}}(t)$.

In the 25 years since the WA paper, attempts have been made to improve their calculation of transition amplitudes by going beyond first-order perturbation theory [5, 6, 7, 8, 9, 10, 12, 11, 13]. In particular, the time-dependent Schrödinger equation that governs the occupation amplitudes of the target states has been integrated numerically from $t = -\infty$ to $t = \infty$ as a set of coupled-channel equations, within a finite set of target basis states. In these calculations, $V_{\text{cl}}(t)$ has been used as the interaction potential. But this clearly goes beyond the justification provided by the work of ABHMW. The coupled-channel equations involve the entire function $V_{\text{cl}}(t)$, not just its on-shell Fourier component. Therefore the relationship between $V_{\text{cl}}(t)$ and $V_{\text{eff}}(t)$ established by ABHMW, which was limited to on-shell Fourier components, cannot be used to justify the use of $V_{\text{cl}}(t)$ in a coupled-channel calculation, or in any calculation that goes beyond first-order perturbation theory.

There are also practical problems associated with the use of $V_{\text{cl}}(t)$ in coupled-channel calculations. As will be shown below, certain matrix elements of $V_{\text{cl}}(t)$ diverge at high bombarding

¹Galetti, Kodama and Nemes [2], and Bertulani *et al* [3] have pointed out difficulties associated with this simple picture.

energy, in proportion to $\log \gamma (= \log(1 - v^2/c^2)^{-1/2})$, a divergence that is unlikely to be a genuine physical effect [12]. Another strange feature of $V_{\text{cl}}(t)$ is that it has matrix elements between pairs of states both of which have zero angular momentum.

Because we believe that the use of $V_{\text{cl}}(t)$ in coupled-channel calculations cannot be justified, we will replace it by $V_{\text{eff}}(t)$, which is more closely related to the fundamental Hamiltonian of the system, and which takes account of the quantization of the electromagnetic field. Our calculation of $V_{\text{eff}}(t)$ follows closely that given by ABHMW, with two exceptions:

- ABHMW calculated only the on-shell Fourier component of $V_{\text{eff}}(t)$, whereas we will calculate the entire time-dependent function.
- The relative motion of the projectile and target was treated quantum-mechanically by ABHMW. Since our attention is focussed on RCE, we will assume that the relative motion corresponds to constant velocity at fixed impact parameter.

In Section 2 we will briefly review the time-dependent picture of Coulomb excitation and introduce $V_{\text{eff}}(t)$. In Section 3 we will present the derivation of $V_{\text{eff}}(t)$, and will compare it to $V_{\text{cl}}(t)$ in Section 4. In Section 5 we will give some numerical comparisons of $V_{\text{eff}}(t)$ and $V_{\text{cl}}(t)$, and in Section 6 we will use $V_{\text{eff}}(t)$ in a coupled-channel calculation of the excitation of states of the giant dipole resonance, and compare the results to those obtained using $V_{\text{cl}}(t)$. Finally in Section 7 we will try to determine the circumstances under which $V_{\text{cl}}(t)$, can be safely used, in place of the more fundamental $V_{\text{eff}}(t)$.

2 Time-dependent analysis of Coulomb excitation and definition of $V_{\text{eff}}(t)$

Data from experiments involving relativistic Coulomb excitation (RCE) are usually analyzed using a time-dependent Schrödinger equation

$$i\hbar \frac{\partial \Psi}{\partial t} = [H_T + V_{\text{cl}}(t)] \Psi \quad (2.1)$$

H_T is the internal target Hamiltonian, and does not depend explicitly on t . The time-dependent interaction $V_{\text{cl}}(t)$ expresses the effect on the target of the classical electromagnetic field due to the projectile. It is an explicit function of time, and of the target degrees of freedom. We want to replace $V_{\text{cl}}(t)$ in equation (2.1) by $V_{\text{eff}}(t)$, which takes account of the quantum nature of the electromagnetic field. Our derivation of $V_{\text{eff}}(t)$ starts with the fundamental interaction between charges and the electromagnetic field, and involves a result from second-order time-dependent perturbation theory. We will now derive this result.

Consider the Schrödinger equation

$$i\hbar \frac{\partial \psi}{\partial t} = [h_0 + v(t)] \psi \quad (2.2)$$

where h_0 and $v(t)$ are unspecified, except that h_0 does not depend explicitly on t . This equation is expressed in the interaction representation by expanding ψ in terms of the normalized eigenstates of h_0 :

$$\psi(t) = \sum_{\gamma} e^{-i\frac{\epsilon_{\gamma}}{\hbar}t} a_{\gamma}(t) \phi_{\gamma}, \quad (2.3)$$

with

$$h_0 \phi_{\gamma} = \epsilon_{\gamma} \phi_{\gamma} \quad (2.4a)$$

$$\langle \phi_{\gamma} | \phi_{\beta} \rangle = \delta_{\gamma,\beta} \quad (2.4b)$$

If ϕ_{α} is the initial state, which existed when $t \rightarrow -\infty$, then

$$a_{\gamma}(-\infty) = \delta_{\gamma,\alpha}. \quad (2.5)$$

The transition probability to state ϕ_{γ} is given by $|a_{\gamma}(+\infty)|^2$.

Because of equation (2.2), the $a_{\alpha}(t)$ obey the set of coupled differential equations:

$$i\hbar \dot{a}_{\gamma}(t) = \sum_{\beta} e^{i\omega_{\gamma\beta}t} [v(t)]_{\gamma\beta} a_{\beta}(t), \quad (2.6a)$$

with

$$[v(t)]_{\gamma\beta} \equiv \langle \phi_{\gamma} | v(t) | \phi_{\beta} \rangle. \quad (2.6b)$$

$\omega_{\gamma\beta}$ is defined in equation (1.1).

The integral equation equivalent to equation(2.6a), incorporating the initial condition (2.5), is

$$a_{\gamma}(t) = \delta_{\gamma,\alpha} + \int_{-\infty}^t \frac{dt'}{i\hbar} \sum_{\beta} e^{i\omega_{\gamma\beta}t'} v_{\gamma\beta}(t') a_{\beta}(t').$$

This can be iterated to develop a perturbation series in powers of $v(t)$:

$$a_{\gamma}(t) = \delta_{\gamma,\alpha} + \int_{-\infty}^t \frac{dt'}{i\hbar} e^{i\omega_{\gamma\alpha}t'} v_{\gamma\alpha}(t') + \sum_{\beta} \int_{-\infty}^t \frac{dt'}{i\hbar} e^{i\omega_{\gamma\beta}t'} v_{\gamma\beta}(t') \int_{-\infty}^{t'} \frac{dt''}{i\hbar} e^{i\omega_{\beta\alpha}t''} v_{\beta\alpha}(t'') + \dots \quad (2.7)$$

The amplitude for a transition from ϕ_{α} at $t = -\infty$ to ϕ_{γ} at $t = \infty$ is $a_{\gamma}(\infty)$. The first three terms of the perturbation series are

$$a_{\gamma}(\infty) = \delta_{\gamma,\alpha} + \int_{-\infty}^{\infty} \frac{dt'}{i\hbar} e^{i\omega_{\gamma\alpha}t'} v_{\gamma\alpha}(t') + \sum_{\beta} \int_{-\infty}^{\infty} \frac{dt'}{i\hbar} e^{i\omega_{\gamma\beta}t'} v_{\gamma\beta}(t') \int_{-\infty}^{t'} \frac{dt''}{i\hbar} e^{i\omega_{\beta\alpha}t''} v_{\beta\alpha}(t''). \quad (2.8)$$

We seek an effective interaction $v_{\text{eff}}(t)$ such that $a_{\gamma}(\infty)$ given by equation (2.8) can also be written as

$$a_{\gamma}(\infty) = \delta_{\gamma,\alpha} + \int_{-\infty}^{\infty} \frac{dt'}{i\hbar} e^{i\omega_{\gamma\alpha}t'} [v_{\text{eff}}(t')]_{\gamma\alpha}. \quad (2.9)$$

This $v_{\text{eff}}(t)$ can be said to incorporate into a single effective interaction the first- and second-order effects of $v(t)$. In our application, these second-order effects correspond to photon exchange between the projectile and target.

3 Calculation of $V_{\text{eff}}(t)$

As explained in the previous sections, our goal is to use the photon-exchange mechanism to calculate an effective time-dependent interaction, $V_{\text{eff}}(t)$, that can be used in coupled-channel calculations of the time-development of target states. Thus $V_{\text{eff}}(t)$ should involve only the target degrees of freedom. In first-order perturbation theory, $V_{\text{eff}}(t)$ should give the same transition amplitude as the one calculated by WA. Thus we expect that the on-shell Fourier components of $V_{\text{eff}}(t)$ should be the same as the corresponding on-shell Fourier components of $V_{\text{cl}}(t)$. However, there is no reason to expect that $V_{\text{eff}}(t)$ and $V_{\text{cl}}(t)$ will be equal. We will show that $V_{\text{eff}}(t)$ calculated from photon-exchange is free of the difficulties of $V_{\text{cl}}(t)$ described in Section 1.

3.1 The Hamiltonian

Since the calculation involves the electromagnetic potentials, we must choose a gauge. We follow the customary practice [14, 15, 16] of using the radiation (or Coulomb) gauge, in which the vector potential is a solenoidal field

$$\nabla \cdot \mathbf{A}(\mathbf{r}, t) = 0. \quad (3.1)$$

Here \mathbf{r} labels points of space relative to an origin at the target center, which we assume to be fixed. We describe the photon field in terms of normal modes, each labelled by a wave vector \mathbf{q} and polarization vector $\hat{\mathbf{e}}_{\mathbf{q},j}$ orthogonal to it. Associated with each \mathbf{q} are *two* polarization vectors $\hat{\mathbf{e}}_{\mathbf{q},1}$ and $\hat{\mathbf{e}}_{\mathbf{q},2}$. The three vectors ($\hat{\mathbf{q}}, \hat{\mathbf{e}}_{\mathbf{q},1}, \hat{\mathbf{e}}_{\mathbf{q},2}$) form an orthonormal coordinate system. The field operator $\mathbf{A}(\mathbf{r}, t)$ is expressed in terms of photon creation and annihilation operators ($a_{\mathbf{q},j}^+(t), a_{\mathbf{q},j}(t)$) by the expansion

$$\mathbf{A}(\mathbf{r}, t) = c \sqrt{\frac{4\pi}{V}} \sum_{\mathbf{q},j} \sqrt{\frac{\hbar}{2qc}} \left[e^{i\mathbf{q}\cdot\mathbf{r}} \hat{\mathbf{e}}_{\mathbf{q},j} a_{\mathbf{q},j}(t) + e^{-i\mathbf{q}\cdot\mathbf{r}} \hat{\mathbf{e}}_{\mathbf{q},j}^* a_{\mathbf{q},j}^+(t) \right]. \quad (3.2)$$

Here V is the quantization volume. The number of modes per unit \mathbf{q} -space volume is $V/8\pi^3$, for each polarization $\hat{\mathbf{e}}_{\mathbf{q},j}$. Since the plane waves that describe the modes are transverse ($\hat{\mathbf{e}}_{\mathbf{q},j} \cdot \hat{\mathbf{q}} = 0$), the solenoidal condition (3.1) is automatically satisfied. With the normalization given in equation (3.2), the ($a_{\mathbf{q},j}^+(t), a_{\mathbf{q},j}(t)$) obey the commutation relations

$$[a_{\mathbf{q},j}(t), a_{\mathbf{q}',j'}^+(t)] = \delta_{\mathbf{q},\mathbf{q}'} \delta_{j,j'} \quad (3.3a)$$

$$[a_{\mathbf{q},j}(t), a_{\mathbf{q}',j'}(t)] = [a_{\mathbf{q},j}^+(t), a_{\mathbf{q}',j'}^+(t)] = 0 \quad (3.3b)$$

Their matrix elements with respect to states with $n_{\mathbf{q},j}$ photons in the mode \mathbf{q}, j are

$$\langle n'_{\mathbf{q},j} | a_{\mathbf{q},j}^+(t) | n_{\mathbf{q},j} \rangle = \delta_{n'_{\mathbf{q},j}, n_{\mathbf{q},j}+1} \sqrt{n_{\mathbf{q},j} + 1} \quad (3.4a)$$

$$\langle n'_{\mathbf{q},j} | a_{\mathbf{q},j}(t) | n_{\mathbf{q},j} \rangle = \delta_{n'_{\mathbf{q},j}, n_{\mathbf{q},j}-1} \sqrt{n_{\mathbf{q},j}} \quad (3.4b)$$

In the radiation gauge, the full Hamiltonian for our system is [15, 14]

$$H = H_T + H_\gamma - \frac{1}{c} \int d^3r (\mathbf{J}_P(\mathbf{r}, t) + \mathbf{J}_T(\mathbf{r})) \cdot \mathbf{A}(\mathbf{r}, \mathbf{t}) + \int d^3r \rho_T(\mathbf{r}) \int d^3\tilde{r} \frac{\rho_P(\tilde{\mathbf{r}}, t)}{|\mathbf{r} - \tilde{\mathbf{r}}|} \quad (3.5)$$

H_T is the target internal Hamiltonian, and

$$H_\gamma \equiv \sum_{\mathbf{q}, j} \hbar c q a_{\mathbf{q}, j}^+(t) a_{\mathbf{q}, j}(t)$$

is the free-field photon Hamiltonian. There is no term in equation (3.5) corresponding to the kinetic energy of relative motion. We are using the usual RCE picture of the projectile moving on a prescribed straight-line classical trajectory, and therefore the projectile-target relative coordinate is not one of the degrees of freedom of the problem. We will see below that, at relativistic projectile velocities, the effect of the projectile on the target is dominated by the center-of-mass motion of the projectile, and thus we neglect any internal degree of freedom of the projectile. The full Hamiltonian (3.5) is of the form used in the time-dependent Schrödinger equation (2.2), with

$$h_0 = H_T + H_\gamma$$

and

$$v(t) = -\frac{1}{c} \int d^3r [(\mathbf{J}_P(\mathbf{r}, t) + \mathbf{J}_T(\mathbf{r})) \cdot \mathbf{A}(\mathbf{r}, \mathbf{t})] + \int d^3r \rho_T(\mathbf{r}) \int d^3\tilde{r} \frac{\rho_P(\tilde{\mathbf{r}}, t)}{|\mathbf{r} - \tilde{\mathbf{r}}|}$$

The eigenstates of h_0 , labelled by ϕ_β , are specified by an internal target eigenstate, and the number of photons, $n_{\mathbf{q}, j}$, in each of the modes \mathbf{q}, j .

3.2 The intermediate states

We are interested in a situation in which neither the initial state ϕ_α nor the final state ϕ_γ have any photons². Thus we exclude bremsstrahlung processes, which we know to be impossible for a projectile moving with constant velocity. Moreover, we assume that every photon absorbed by the target at time t was emitted by the projectile at an earlier time t' , and every photon emitted by the target at time t will be absorbed by the projectile at a later time t' ³. Then consideration of processes up to second order in the interaction between the electromagnetic field and the projectile and target charge requires the following states:

1. ϕ_α is the initial target state \times the photon vacuum
2. ϕ_γ is the final target state \times the photon vacuum
3. ϕ_{β_1} is the initial target state \times one photon in the mode \mathbf{q}, j

²To keep the notation simple, we use $\phi_{\alpha, \gamma}$ to label target states, or target states in the presence of the photon vacuum. We believe that the presence or absence of the vacuum will be clear in all situations.

³In particular, we do not imagine that a photon absorbed by the target was emitted by the target. Such target emission-absorption processes contribute to the renormalization of the target mass, and are not considered here.

4. ϕ_{β_2} is the final target state \times one photon in the mode \mathbf{q}, j

The last term in equation (3.5), which does not involve the photon degrees of freedom, is a direct coupling between the initial and final target states $\phi_{\alpha, \gamma}$, and so provides a non-zero $v_{\gamma\alpha}(t)$. However, the terms in equation (3.5) linear in $\mathbf{A}(\mathbf{r}, t)$ are also linear in the photon creation and annihilation operators. These can only connect states in which the number of photons in some mode \mathbf{q}, j changes by one. Thus ϕ_α and ϕ_γ can be connected by the current-photon interaction terms to the states ϕ_{β_1} and ϕ_{β_2} . These processes are illustrated in Figure 1.

To emphasize the distinction between states ϕ_{β_1} and ϕ_{β_2} , we re-write equation (2.8):

$$\begin{aligned} a_\gamma(\infty) &= \delta_{\gamma, \alpha} + \int_{-\infty}^{\infty} \frac{dt'}{i\hbar} e^{i\omega_\gamma \alpha t'} v_{\gamma\alpha}(t') + \sum_{\beta_1} \int_{-\infty}^{\infty} \frac{dt'}{i\hbar} e^{i\omega_{\gamma\beta_1} t'} v_{\gamma\beta_1}(t') \int_{-\infty}^{t'} \frac{dt''}{i\hbar} e^{i\omega_{\beta_1\alpha} t''} v_{\beta_1\alpha}(t'') \\ &+ \sum_{\beta_2} \int_{-\infty}^{\infty} \frac{dt'}{i\hbar} e^{i\omega_{\gamma\beta_2} t'} v_{\gamma\beta_2}(t') \int_{-\infty}^{t'} \frac{dt''}{i\hbar} e^{i\omega_{\beta_2\alpha} t''} v_{\beta_2\alpha}(t'') \end{aligned} \quad (3.6)$$

It will be convenient to interchange the order of the t' and t'' integrations in the last line of equation (3.6), and then re-label these variables:

$$\begin{aligned} \int_{-\infty}^{\infty} \frac{dt'}{i\hbar} e^{i\omega_{\gamma\beta_2} t'} v_{\gamma\beta_2}(t') \int_{-\infty}^{t'} \frac{dt''}{i\hbar} e^{i\omega_{\beta_2\alpha} t''} v_{\beta_2\alpha}(t'') &= \int_{-\infty}^{\infty} \frac{dt''}{i\hbar} e^{i\omega_{\beta_2\alpha} t''} v_{\beta_2\alpha}(t'') \int_{t''}^{\infty} \frac{dt'}{i\hbar} e^{i\omega_{\gamma\beta_2} t'} v_{\gamma\beta_2}(t') \\ &= \int_{-\infty}^{\infty} \frac{dt'}{i\hbar} e^{i\omega_{\beta_2\alpha} t'} v_{\beta_2\alpha}(t') \int_{t'}^{\infty} \frac{dt''}{i\hbar} e^{i\omega_{\gamma\beta_2} t''} v_{\gamma\beta_2}(t''), \end{aligned}$$

so that equation (3.6) can be written

$$\begin{aligned} a_\gamma(\infty) &= \delta_{\gamma, \alpha} + \int_{-\infty}^{\infty} \frac{dt'}{i\hbar} e^{i\omega_\gamma \alpha t'} v_{\gamma\alpha}(t') + \sum_{\beta_1} \int_{-\infty}^{\infty} \frac{dt'}{i\hbar} e^{i\omega_{\gamma\beta_1} t'} v_{\gamma\beta_1}(t') \int_{-\infty}^{t'} \frac{dt''}{i\hbar} e^{i\omega_{\beta_1\alpha} t''} v_{\beta_1\alpha}(t'') \\ &+ \sum_{\beta_2} \int_{-\infty}^{\infty} \frac{dt'}{i\hbar} e^{i\omega_{\beta_2\alpha} t'} v_{\beta_2\alpha}(t') \int_{t'}^{\infty} \frac{dt''}{i\hbar} e^{i\omega_{\gamma\beta_2} t''} v_{\gamma\beta_2}(t''). \end{aligned}$$

If we compare this to equation (2.9), we get

$$\begin{aligned} [v_{\text{eff}}(t')]_{\gamma\alpha} &= v_{\gamma\alpha}(t') + \sum_{\beta_1} v_{\gamma\beta_1}(t') \int_{-\infty}^{t'} \frac{dt''}{i\hbar} e^{i\omega_{\beta_1\alpha}(t''-t')} v_{\beta_1\alpha}(t'') \\ &+ \sum_{\beta_2} v_{\beta_2\alpha}(t') \int_{t'}^{\infty} \frac{dt''}{i\hbar} e^{i\omega_{\gamma\beta_2}(t''-t')} v_{\gamma\beta_2}(t''). \end{aligned} \quad (3.7)$$

3.3 Photon-current couplings

The direct term $v_{\gamma\alpha}(t)$ in equation (3.7) is the instantaneous density-density interaction. The part of the Hamiltonian needed for the second-order terms in equation(3.7) is $-(\mathbf{J}_P + \mathbf{J}_T) \cdot \mathbf{A}/c$.

Let us first consider the β_1 sum, which corresponds to the process illustrated in Figure 1(a). This sum over β_1 is actually an integration over all photon modes:

$$\sum_{\beta_1} \longrightarrow \frac{V}{(2\pi)^3} \sum_{j=1,2} \int d^3q \quad (3.8)$$

Reference to Figure 1 shows that $\omega_{\beta_1\alpha}$ and $\omega_{\gamma\beta_2}$ are given by

$$\omega_{\beta_1\alpha} = (\hbar cq + \epsilon_\alpha - \epsilon_\alpha)/\hbar = cq \quad (3.9a)$$

$$\omega_{\gamma\beta_2} = (\epsilon_\gamma - \hbar cq - \epsilon_\gamma)/\hbar = -cq \quad (3.9b)$$

Using equations (3.2), (3.4a,3.4b), (3.5), (3.8) and (3.9a), we find that the β_1 sum of equation (3.7) becomes

$$\frac{V}{(2\pi)^3} \left(\sqrt{\frac{4\pi}{V}} \right)^2 \sum_{j=1,2} \int d^3q \frac{\hbar}{2qc} \int e^{i\mathbf{q}\cdot\mathbf{r}} \hat{\mathbf{e}}_{\mathbf{q},j} \cdot [\mathbf{J}_T(\mathbf{r})]_{\gamma\alpha} d^3r \int_{-\infty}^{t'} \frac{dt''}{i\hbar} e^{icq(t''-t')} \int e^{-i\mathbf{q}\cdot\mathbf{r}} \hat{\mathbf{e}}_{\mathbf{q},j}^* \cdot \mathbf{J}_P(\mathbf{r}, t'') d^3r \quad (3.10)$$

To determine $\mathbf{J}_P(\mathbf{r}, t)$, we start in the projectile rest-frame in which \tilde{t} labels the time and $\tilde{\mathbf{r}}$ labels points with respect to the projectile center. Let $\tilde{\rho}_P(\tilde{\mathbf{r}})$ and $\tilde{\mathbf{J}}_P(\tilde{\mathbf{r}})$ be the projectile charge and current densities measured in the projectile rest frame. Then if the projectile moves so that its center is located relative to the target center by

$$\mathbf{r} = b\hat{\mathbf{y}} + vt\hat{\mathbf{z}}, \quad (3.11)$$

an observer at the target center will observe projectile charge and current densities given by

$$\rho_P(\mathbf{r}, t) = \gamma \left[\tilde{\rho}_P(\tilde{\mathbf{r}}) + \frac{v}{c^2} [\tilde{\mathbf{J}}_P]_z(\tilde{\mathbf{r}}) \right] \quad (3.12a)$$

$$[\tilde{\mathbf{J}}_P]_{x,y}(\mathbf{r}, t) = [\tilde{\mathbf{J}}_P]_{x,y}(\tilde{\mathbf{r}}) \quad (3.12b)$$

$$[\tilde{\mathbf{J}}_P]_z(\mathbf{r}, t) = \gamma \left[[\tilde{\mathbf{J}}_P]_z(\tilde{\mathbf{r}}) + v\tilde{\rho}_P(\tilde{\mathbf{r}}) \right], \quad (3.12c)$$

with

$$\tilde{x} = x \quad (3.13a)$$

$$\tilde{y} = y - b \quad (3.13b)$$

$$\tilde{z} = \gamma(z - vt) \quad (3.13c)$$

$$\gamma \equiv \left(1 - \frac{v^2}{c^2} \right)^{-\frac{1}{2}} \quad (3.13d)$$

Our focus is on the regime in which $v \sim c$. Then v will be much larger than the internal speeds of the projectile nucleons, so that the projectile current density seen by the target is dominated by the center-of-mass velocity of the projectile:

$$\begin{aligned} [\tilde{\mathbf{J}}_P]_z(\mathbf{r}, t) &\sim \gamma v \tilde{\rho}_P(\tilde{\mathbf{r}}) \\ &= \gamma v \tilde{\rho}_P(x, y - b, \gamma(z - vt)) \end{aligned} \quad (3.14a)$$

$$[\tilde{\mathbf{J}}_P]_{x,y}(\mathbf{r}, t) \ll [\tilde{\mathbf{J}}_P]_z(\mathbf{r}, t) \quad (3.14b)$$

$$\begin{aligned} \rho_P(\mathbf{r}, t) &\sim \gamma \tilde{\rho}_P(\tilde{\mathbf{r}}) \\ &= \gamma \tilde{\rho}_P(x, y - b, \gamma(z - vt)). \end{aligned} \quad (3.14c)$$

We will make the further assumption that the projectile charge density is spherically symmetric in its own rest frame⁴:

$$\tilde{\rho}_P(\tilde{x}, \tilde{y}, \tilde{z}) = \tilde{\rho}_P\left(\sqrt{\tilde{x}^2 + \tilde{y}^2 + \tilde{z}^2}\right) \quad (3.15)$$

Then the \mathbf{r} integrals needed in equation (3.10) can be easily performed, and we find⁵ that the total of the β_1 , β_2 sums in equation (3.7) is given by

$$\begin{aligned} P(t) \equiv & -\frac{2v}{\pi c^2} \int \frac{d^3q}{q_\perp^2 + \left(\frac{q_z}{\gamma}\right)^2} e^{-iq_z vt'} \int_0^\infty \tilde{r}^2 d\tilde{r} \tilde{\rho}_P(\tilde{r}) j_0\left(\tilde{r} \sqrt{q_\perp^2 + \left(\frac{q_z}{\gamma}\right)^2}\right) \\ & \times \int d^3r \left[[\mathbf{J}_T]_z - \frac{(\mathbf{J}_T \cdot \mathbf{q}) q_z}{q^2} \right]_{\gamma\alpha} e^{i\mathbf{q}_\perp \cdot (\mathbf{r} - \mathbf{b})}. \end{aligned}$$

Furthermore, we note that q_z and q_\perp play different roles in this expression, and so we separate them in d^3q and write $d^3q = d^2q_\perp dq_z$, and we replace the variable q_z by the combination $vq_z \equiv \omega$. Then the photon-mediated part of the effective target interaction becomes

$$\begin{aligned} P(t) = & -\frac{2}{\pi c^2} \int_{-\infty}^\infty d\omega e^{-i\omega t'} \int \frac{d^2q}{q_\perp^2 + \left(\frac{\omega}{\gamma v}\right)^2} \int_0^\infty \tilde{r}^2 d\tilde{r} \tilde{\rho}_P(\tilde{r}) j_0\left(\tilde{r} \sqrt{q_\perp^2 + \left(\frac{\omega}{\gamma v}\right)^2}\right) \\ & \times \int d^3r \left[[\mathbf{J}_T]_z - \frac{(\mathbf{J}_T \cdot \mathbf{q}) \omega}{q^2 v} \right]_{\gamma\alpha} e^{i\mathbf{q}_\perp \cdot (\mathbf{r} - \mathbf{b})}. \end{aligned} \quad (3.16)$$

3.4 The instantaneous density-density interaction

The last term in H of equation (3.5) can be evaluated starting with

$$\frac{1}{|\mathbf{r} - \tilde{\mathbf{r}}|} = \lim_{\eta \rightarrow 0} \frac{e^{-\eta|\mathbf{r} - \tilde{\mathbf{r}}|}}{|\mathbf{r} - \tilde{\mathbf{r}}|} = \frac{1}{2\pi^2} \lim_{\eta \rightarrow 0} \int d^3q \frac{e^{i\mathbf{q} \cdot (\mathbf{r} - \tilde{\mathbf{r}})}}{q^2 + \eta^2}.$$

If we use this representation of $1/|\mathbf{r} - \tilde{\mathbf{r}}|$ in equation (3.5), and express $\rho_P(\tilde{\mathbf{r}})$ in terms of $\tilde{\rho}_P(\tilde{\mathbf{r}})$ using equation (3.14c), we get

$$\begin{aligned} & \int d^3r \rho_T(\mathbf{r}) \int d^3\tilde{r} \frac{\rho_P(\tilde{\mathbf{r}}, t)}{|\mathbf{r} - \tilde{\mathbf{r}}|} = \\ & \frac{2}{\pi v} \int_{-\infty}^\infty d\omega e^{-i\omega t} \int \frac{d^2q_\perp}{q_\perp^2 + \left(\frac{\omega}{v}\right)^2} \times \int_0^\infty \tilde{r}^2 d\tilde{r} \tilde{\rho}_P(\tilde{r}) j_0\left(\tilde{r} \sqrt{q_\perp^2 + \left(\frac{\omega}{v}\right)^2}\right) \int d^3r \rho_T(\mathbf{r}) e^{i\mathbf{q} \cdot (\mathbf{r} - \mathbf{b})} \end{aligned} \quad (3.17)$$

⁴We will see in Section 6 that the calculated results are insensitive to the radial dependence of the projectile density. This is because the most important b values are greater than the projectile radius.

⁵Some algebraic details are given in Appendix A.

3.5 The effective potential

We now combine equations (3.5), (3.16) and (3.17) to obtain the total effective target Hamiltonian. The time dependencies of both (3.16) and (3.17) are expressed as Fourier transforms of functions of ω , and thus we write

$$H = H_{\text{T}} + V_{\text{eff}}(t) \quad (3.18a)$$

with

$$V_{\text{eff}}(t) = \frac{\hbar}{2\pi} \int_{-\infty}^{\infty} d\omega e^{-i\omega t} V_{\text{eff}}^{\text{F.T.}}(\omega) \quad (3.18b)$$

$$\begin{aligned} [V_{\text{eff}}^{\text{F.T.}}(\omega)]_{\gamma\alpha} &= -\frac{4}{\hbar c^2} \int \frac{d^2 q_{\perp}}{q_{\perp}^2 + \left(\frac{\omega}{\gamma v}\right)^2} \int_0^{\infty} \tilde{r}^2 d\tilde{r} \tilde{\rho}_{\text{P}}(\tilde{r}) j_0 \left(\tilde{r} \sqrt{q_{\perp}^2 + \left(\frac{\omega}{\gamma v}\right)^2} \right) \\ &\times \int d^3 r e^{i\mathbf{q}\cdot(\mathbf{r}-\mathbf{b})} \left([\mathbf{J}_{\text{T}}(\mathbf{r})]_z - \frac{(\mathbf{J}_{\text{T}}(\mathbf{r}) \cdot \mathbf{q})\omega}{\left(q_{\perp}^2 + \left(\frac{\omega}{v}\right)^2\right)v} \right)_{\gamma\alpha} \\ &+ \frac{4}{\hbar v} \int \frac{d^2 q_{\perp}}{q_{\perp}^2 + \left(\frac{\omega}{v}\right)^2} \times \int_0^{\infty} \tilde{r}^2 d\tilde{r} \tilde{\rho}_{\text{P}}(\tilde{r}) j_0 \left(\tilde{r} \sqrt{q_{\perp}^2 + \left(\frac{\omega}{\gamma v}\right)^2} \right) \\ &\times \int d^3 r [\rho_{\text{T}}(\mathbf{r})]_{\gamma\alpha} e^{i\mathbf{q}\cdot(\mathbf{r}-\mathbf{b})} \end{aligned} \quad (3.18c)$$

This equation can be simplified by making use of the following formulae:

$$\frac{1}{q_{\perp}^2 + \left(\frac{\omega}{\gamma v}\right)^2} \cdot \frac{1}{q_{\perp}^2 + \left(\frac{\omega}{v}\right)^2} = \frac{c^2}{\omega^2} \left[\frac{1}{q_{\perp}^2 + \left(\frac{\omega}{\gamma v}\right)^2} - \frac{1}{q_{\perp}^2 + \left(\frac{\omega}{v}\right)^2} \right] \quad (3.19a)$$

$$\begin{aligned} \int d^3 r [\rho_{\text{T}}(\mathbf{r})]_{\gamma\alpha} f(\mathbf{r}) &= -\frac{1}{i\omega\gamma\alpha} \int d^3 r (\nabla \cdot [\mathbf{J}_{\text{T}}(\mathbf{r})]_{\gamma\alpha}) f(\mathbf{r}) \\ &= \frac{1}{i\omega\gamma\alpha} \int d^3 r [\mathbf{J}_{\text{T}}(\mathbf{r})]_{\gamma\alpha} \cdot \nabla f(\mathbf{r}) \end{aligned} \quad (3.19b)$$

$$\int \frac{d^2 \mathbf{q}_{\perp}}{q_{\perp}^2 + \left(\frac{\omega}{\gamma v}\right)^2} e^{i\mathbf{q}_{\perp} \cdot (\boldsymbol{\rho} - \mathbf{b})} j_0 \left(\tilde{r} \sqrt{q_{\perp}^2 + \left(\frac{\omega}{\gamma v}\right)^2} \right) = 2\pi K_0 \left(\frac{|\omega| |\boldsymbol{\rho} - \mathbf{b}|}{\gamma v} \right) \quad (3.19c)$$

$$\begin{aligned} \int \frac{d^2 \mathbf{q}_{\perp}}{q_{\perp}^2 + \left(\frac{\omega}{v}\right)^2} e^{i\mathbf{q}_{\perp} \cdot (\boldsymbol{\rho} - \mathbf{b})} j_0 \left(\tilde{r} \sqrt{q_{\perp}^2 + \left(\frac{\omega}{\gamma v}\right)^2} \right) &= 2\pi K_0 \left(\frac{|\omega| |\boldsymbol{\rho} - \mathbf{b}|}{v} \right) \\ &\times j_0 \left(i\tilde{r} \frac{|\omega|}{c} \right). \end{aligned} \quad (3.19d)$$

Equation (3.19b) uses charge conservation and the finite extent of the target charge distribution. Equations (3.19b and 3.19d), which are proven in Appendix B, are valid when $\tilde{r} < |\boldsymbol{\rho} - \mathbf{b}|$.

This condition is satisfied because of our assumption b is large enough so that the projectile and target never overlap.

The simplification of equation (3.18c) leads to

$$\begin{aligned}
[V_{\text{eff}}^{\text{F.T.}}(\omega)]_{\gamma\alpha} = & -\frac{2Z_{\text{P}}e}{\hbar c^2} \int d^3r [\mathbf{J}_{\text{T}}(\mathbf{r})]_{\gamma\alpha} \cdot \left(\hat{\mathbf{z}} + \frac{ic^2}{v\omega} \nabla \right) K_0 \left(\frac{|\omega||\boldsymbol{\rho} - \mathbf{b}|}{\gamma v} \right) e^{i\frac{\omega}{v}z} \\
& -\frac{8\pi i}{\hbar v\omega_{\gamma\alpha}} \left(1 - \frac{\omega_{\gamma\alpha}}{\omega} \right) \int_0^\infty \tilde{r}^2 d\tilde{r} j_0 \left(i\tilde{r} \frac{\omega}{c} \right) \tilde{\rho}_{\text{P}}(\tilde{r}) \\
& \times \int d^3r [\mathbf{J}_{\text{T}}(\mathbf{r})]_{\gamma\alpha} \cdot \nabla K_0 \left(\frac{|\omega||\boldsymbol{\rho} - \mathbf{b}|}{v} \right) e^{i\frac{\omega}{v}z}.
\end{aligned} \tag{3.20}$$

Equations (3.18b) and (3.20) give the time-dependent effective potential which we propose to use in coupled-channel analyses of RCE.

3.6 $V_{\text{eff}}(t)$ as an interaction potential

Our goal in the previous sections has been the calculation of the matrix elements of $V_{\text{eff}}(t)$ at a given time t . This quantity involved photons emitted by the projectile at earlier times $t' < t$, and photons absorbed by the projectile at later times $t'' > t$. An essential assumption of this calculation was that the high projectile speed implied that the projectile current density was dominated by the center-of-mass motion of the projectile, which is assumed to be constant throughout the collision. Thus the same expression for $V_{\text{eff}}(t)$ can be used throughout the collision, and the result presented in equations (3.18b) and (3.20) can be used in any study of the time-development of the target wave-function under the influence of this time-dependent external field. However, if the projectile current density were to change significantly at each interaction with the electromagnetic field, this treatment would be invalid. In this situation, it would be necessary to include both the projectile and target internal degrees of freedom into the calculation on the same footing.

It should be noted that, at any given time t , many different photon modes may be excited, due to projectile and/or target interactions with the electromagnetic field at earlier times t' . We only assume that those modes excited by the projectile will de-excited by the target, and those modes excited by the target will be de-excited by the projectile.

4 Comparison of V_{eff} and V_{cl}

4.1 The classical electromagnetic field of the moving projectile.

At time t and at point $\boldsymbol{\rho}, z$ of the target, the scalar and vector potentials of the classical electromagnetic field due to an inert, spherically-symmetric, moving projectile are [16]

$$\varphi_{\text{cl}}(\boldsymbol{\rho}, z, t) = \frac{Z_{\text{P}}e\gamma}{\sqrt{(\boldsymbol{\rho} - \mathbf{b})^2 + \gamma^2(z - vt)^2}} \tag{4.1a}$$

$$\mathbf{A}_{\text{cl}}(\boldsymbol{\rho}, z, t) = \frac{v}{c} \varphi_{\text{cl}}^{\text{ret}}(\boldsymbol{\rho}, z, t) \hat{\mathbf{z}}, \tag{4.1b}$$

which introduce time-dependent terms

$$V_{\text{cl}}(t) = \int d^3r \left[\rho_{\text{T}}(\mathbf{r})\varphi_{\text{cl}}(\mathbf{r}, t) - \frac{1}{c} \mathbf{J}_{\text{T}}(\mathbf{r}) \cdot \mathbf{A}_{\text{cl}}(\mathbf{r}, t) \right] \quad (4.2)$$

into the target Hamiltonian. This interaction serves as the $v(t)$ of equation (2.2).

4.2 On-shell matrix elements of $V_{\text{eff}}(t)$ and $V_{\text{cl}}(t)$

Equation (3.18b) expresses $V_{\text{eff}}(t)$ as the Fourier transform of the function specified in equation in (3.20). It will be convenient to compare $V_{\text{eff}}(t)$ and $V_{\text{cl}}(t)$ in terms of their Fourier transforms. Thus we calculate

$$\begin{aligned} \varphi_{\text{cl}}^{\text{F.T.}}(\boldsymbol{\rho}, z, \omega) &\equiv \int_{-\infty}^{\infty} \frac{dt}{\hbar} e^{i\omega t} \varphi_{\text{cl}}(\boldsymbol{\rho}, z, t) = \frac{\gamma Z_{\text{P}} e}{\hbar} \int_{-\infty}^{\infty} \frac{e^{i\omega t} dt}{\sqrt{(\boldsymbol{\rho} - \mathbf{b})^2 + \gamma^2(z - vt)^2}} \\ &= \frac{2Z_{\text{P}} e}{v} e^{i\frac{\omega}{v}z} K_0 \left(\frac{|\omega| |\boldsymbol{\rho} - \mathbf{b}|}{\gamma v} \right). \end{aligned} \quad (4.3)$$

Then the Fourier transform of the matrix element $[V_{\text{cl}}(t)]_{\gamma\alpha}$ can be written

$$\begin{aligned} [V_{\text{cl}}^{\text{F.T.}}(\omega)]_{\gamma\alpha} &\equiv \int_{-\infty}^{\infty} \frac{dt}{\hbar} e^{i\omega t} [V_{\text{cl}}(t)]_{\gamma\alpha} \\ &= \frac{2Z_{\text{P}} e}{\hbar v} \int d^3r e^{i\frac{\omega}{v}z} K_0 \left(\frac{|\omega| |\boldsymbol{\rho} - \mathbf{b}|}{\gamma v} \right) \left[\rho_{\text{T}} - \frac{v}{c^2} [\mathbf{J}_{\text{T}}]_z \right]_{\gamma\alpha} \end{aligned} \quad (4.4)$$

If we use equation (3.19b) in equation (4.4), we get an expression for $[V_{\text{cl}}^{\text{F.T.}}(\omega)]_{\gamma\alpha}$ in terms of $[\mathbf{J}_{\text{T}}(\mathbf{r})]_{\gamma\alpha}$ alone:

$$[V_{\text{cl}}^{\text{F.T.}}(\omega)]_{\gamma\alpha} = -\frac{2Z_{\text{P}} e}{\hbar c^2} \int d^3r [\mathbf{J}_{\text{T}}(\mathbf{r})]_{\gamma\alpha} \cdot \left[\hat{\mathbf{z}} + \frac{ic^2}{v\omega_{\gamma\alpha}} \nabla \right] e^{i\frac{\omega}{v}z} K_0 \left(\frac{|\omega| |\boldsymbol{\rho} - \mathbf{b}|}{\gamma v} \right). \quad (4.5)$$

Comparison of equations (4.5) and (3.20) shows that

$$[V_{\text{eff}}^{\text{F.T.}}(\omega_{\gamma\alpha})]_{\gamma\alpha} = [V_{\text{cl}}^{\text{F.T.}}(\omega_{\gamma\alpha})]_{\gamma\alpha}. \quad (4.6)$$

Thus, in first-order perturbation theory calculations, $V_{\text{cl}}(t)$ and $V_{\text{eff}}(t)$ can be used interchangeably.

The previous derivation of equation (4.6) has used the assumption that the relative motion of projectile and target is the straight-line classical trajectory commonly used in RCE. However the result is more general. Comparison of ABHMW with the work of Biedenharn, McHale and Thaler [17] shows that an analagous result can be proven when the relative motion is governed by a Coulomb-distorted wave function.

4.3 Comparison of high bombarding energy limits of V_{cl} and V_{eff}

At high bombarding energy, where $v \sim c$, the main bombarding energy dependence enters $V_{\text{cl}}(t)$ and $V_{\text{eff}}(t)$ via the γ -dependencies exhibited by equations (3.20) and (4.5). Since

$$\lim_{\substack{\gamma \rightarrow \infty \\ v \rightarrow c}} K_0 \left(\frac{|\omega||\boldsymbol{\rho} - \mathbf{b}|}{\gamma v} \right) = -\log \left(\frac{|\omega||\boldsymbol{\rho} - \mathbf{b}|}{\gamma v} \right) \xrightarrow{\gamma \rightarrow \infty} \log \gamma,$$

we have

$$\begin{aligned} \lim_{\substack{\gamma \rightarrow \infty \\ v \rightarrow c}} [V_{\text{cl}}^{\text{F.T.}}(\omega)]_{\gamma\alpha} &= -\frac{2Z_{\text{P}}e}{\hbar c^2} \log \gamma \int d^3r [\mathbf{J}_{\text{T}}(\mathbf{r})]_{\gamma\alpha} \cdot \left[\hat{\mathbf{z}} + \frac{ic^2}{v\omega_{\gamma\alpha}} \nabla \right] e^{i\frac{\omega}{v}z} \\ &= -\frac{2Z_{\text{P}}e}{\hbar c^2} \log \gamma \left(1 - \frac{\omega}{\omega_{\gamma\alpha}} \frac{c^2}{v^2} \right) \int d^3r [\mathbf{J}_{\text{T}}(\mathbf{r})]_{\gamma\alpha} \cdot \hat{\mathbf{z}} e^{i\frac{\omega}{v}z} \\ &\xrightarrow{v \rightarrow c} -\frac{2Z_{\text{P}}e}{\hbar c^2} \log \gamma \left(1 - \frac{\omega}{\omega_{\gamma\alpha}} \right) \int d^3r [\mathbf{J}_{\text{T}}(\mathbf{r})]_{\gamma\alpha} \cdot \hat{\mathbf{z}} e^{i\frac{\omega}{v}z} \end{aligned} \quad (4.7)$$

Since the ϕ dependence of $[\mathbf{J}_{\text{T}}(\mathbf{r})]_{\gamma\alpha} \cdot \hat{\mathbf{z}}$ is given by $e^{i(M_{\gamma} - M_{\alpha})\phi}$, the axial symmetry of $e^{i\frac{\omega}{v}z}$ implies that the integral in (4.7) vanishes unless $M_{\gamma} - M_{\alpha} (\equiv \mu) = 0$. Thus we can have a $\log \gamma$ divergence of $[V_{\text{cl}}^{\text{F.T.}}(\omega)]_{\gamma\alpha}$ if $\omega \neq \omega_{\gamma\alpha}$ and $M_{\gamma} = M_{\alpha}$. The effect of this divergence on high bombarding energy cross-sections was noted in Reference [12], and is illustrated in Section 6 below.

The high-bombarding-energy behavior of $[V_{\text{eff}}^{\text{F.T.}}(\omega)]_{\gamma\alpha}$ is quite different. The last two lines of equation (3.20) are independent of γ , and so obviously do not diverge as $\gamma \rightarrow \infty$. The high- γ behavior of the first line is dominated by

$$\begin{aligned} &\lim_{\substack{\gamma \rightarrow \infty \\ v \rightarrow c}} -\frac{2Z_{\text{P}}e}{\hbar c^2} \log \gamma \int d^3r [\mathbf{J}_{\text{T}}(\mathbf{r})]_{\gamma\alpha} \cdot \left[\hat{\mathbf{z}} + \frac{ic^2}{v\omega} \nabla \right] e^{i\frac{\omega}{v}z} \\ &= -\frac{2Z_{\text{P}}e}{\hbar c^2} \log \gamma \left(1 - \frac{c^2}{v^2} \right) \int d^3r [\mathbf{J}_{\text{T}}(\mathbf{r})]_{\gamma\alpha} \cdot \hat{\mathbf{z}} e^{i\frac{\omega}{v}z} \\ &= \frac{2Z_{\text{P}}e}{\hbar v^2} \frac{\log \gamma}{\gamma^2} \int d^3r [\mathbf{J}_{\text{T}}(\mathbf{r})]_{\gamma\alpha} \cdot \hat{\mathbf{z}} e^{i\frac{\omega}{v}z} \end{aligned}$$

The factor of $1/\gamma^2$ overpowers the $\log \gamma$ divergence, and the matrix element $[V_{\text{eff}}^{\text{F.T.}}(\omega)]_{\gamma\alpha}$ is seen to be finite at arbitrarily high bombarding energy.

4.4 Multipole expansions of $V_{\text{eff}}^{\text{F.T.}}(\omega)$ and $V_{\text{cl}}^{\text{F.T.}}(\omega)$

It is illuminating to express equations(3.20) and (4.5) in terms of the multipole expansion given by WA:

$$e^{i\frac{\omega}{v}z} K_0 \left(\frac{|\omega||\boldsymbol{\rho} - \mathbf{b}|}{\gamma v} \right) = \sum_{\mu} e^{-i\mu\phi_{\text{b}}} K_{\mu} \left(\frac{|\omega|b}{\gamma v} \right) \sum_{\lambda} \mathcal{G}_{\lambda\mu} j_{\lambda} \left(\frac{|\omega|}{c} r \right) Y_{\mu}^{\lambda}(\hat{\mathbf{r}}) \quad (4.8a)$$

with $\mathcal{G}_{\lambda\mu}$ defined by

$$\begin{aligned} \mathcal{G}_{\lambda\mu} &\equiv \frac{i^{\lambda+\mu}}{(2\gamma)^\mu} \left(\frac{\omega}{|\omega|}\right)^{\lambda-\mu} \left(\frac{c}{v}\right)^\lambda \sqrt{4\pi(2\lambda+1)(\lambda-\mu)! (\lambda+\mu)!} \\ &\times \sum_n \frac{1}{(2\gamma)^{2n} (n+\mu)! n! (\lambda-\mu-2n)!} \end{aligned} \quad (4.8b)$$

To expand the third line of equation (3.20), we also need the $\gamma \rightarrow 1$ limits of equations (4.8a, 4.8b). To perform these limits, without affecting the value of v , we allow $c \rightarrow \infty$, and obtain

$$\begin{aligned} e^{i\frac{\omega}{v}z} K_0 \left(\frac{|\omega| |\boldsymbol{\rho} - \mathbf{b}|}{v} \right) &= \sum_\mu e^{-i\mu\phi_b} K_\mu \left(\frac{|\omega|b}{v} \right) \sum_\lambda \sqrt{\frac{4\pi}{2\lambda+1}} \frac{i^{\lambda+\mu}}{\sqrt{(\lambda+\mu)! (\lambda-\mu)!}} \\ &\times \left(\frac{|\omega|}{\omega} \right)^{\lambda-\mu} \left(\frac{\omega r}{v} \right)^\lambda Y_\mu^\lambda(\hat{\mathbf{r}}). \end{aligned} \quad (4.9)$$

If we apply equations (4.8a) and (4.9) to equation (3.20), we find

$$[V_{\text{eff}}^{\text{F.T.}}(\omega)]_{\gamma\alpha} = \frac{2Z_P e}{\hbar v} \sum_\mu e^{-i\mu\phi_b} \cdot \sum_{\lambda=|\mu|}^{\infty} \left[(X_\mu^\lambda(E) + X_\mu^\lambda(M)) K_\mu \left(\frac{|\omega|b}{\gamma v} \right) + X_\mu^\lambda(S) K_\mu \left(\frac{|\omega|b}{v} \right) \right], \quad (4.10)$$

where

$$\begin{aligned} X_\mu^\lambda(E) &\equiv \frac{iv}{c\hbar\omega} \left[\frac{\mathcal{G}_{\lambda-1,\mu}}{\lambda} \sqrt{\frac{\lambda^2 - \mu^2}{(2\lambda+1)(2\lambda-1)}} + \frac{\mathcal{G}_{\lambda+1,\mu}}{\lambda+1} \sqrt{\frac{(\lambda+1)^2 - \mu^2}{(2\lambda+1)(2\lambda+3)}} \right] \\ &\times \int d^3r [\mathbf{J}_T]_{\gamma\alpha}(\mathbf{r}) \cdot (\nabla \times \mathbf{L}) j_\lambda \left(\frac{\omega}{c} r \right) Y_\mu^\lambda(\hat{\mathbf{r}}) \end{aligned} \quad (4.11a)$$

$$X_\mu^\lambda(M) \equiv -\frac{v\mu}{c^2\hbar} \frac{\mathcal{G}_{\lambda,\mu}}{\lambda(\lambda+1)} \times \int d^3r [\mathbf{J}_T]_{\gamma\alpha}(\mathbf{r}) \cdot \mathbf{L} j_\lambda \left(\frac{\omega}{c} r \right) Y_\mu^\lambda(\hat{\mathbf{r}}) \quad (4.11b)$$

$$\begin{aligned} X_\mu^\lambda(S) &\equiv \left(1 - \frac{\omega_{\gamma\alpha}}{\omega}\right) \frac{4\pi}{Z_P e} \int_0^\infty \tilde{r}^2 d\tilde{r} \tilde{\rho}_P(\tilde{r}) j_0 \left(i\tilde{r} \frac{\omega}{c} \right) \sqrt{\frac{4\pi}{2\lambda+1}} \frac{i^{\lambda+\mu}}{\sqrt{(\lambda+\mu)! (\lambda-\mu)!}} \\ &\times \left(\frac{|\omega|}{\omega} \right)^{\lambda-\mu} \frac{1}{i\omega_{\gamma\alpha}} \left(\frac{\omega}{v} \right)^\lambda \times \int d^3r [\mathbf{J}_T(\mathbf{r})]_{\gamma\alpha} \cdot \nabla r^\lambda Y_\mu^\lambda(\hat{\mathbf{r}}) \end{aligned} \quad (4.11c)$$

On the other hand, substituting equation (4.8a) into equation (4.5) gives

$$[V_{\text{cl}}^{\text{F.T.}}(\omega)]_{\gamma\alpha} = \frac{2Z_P e}{\hbar v} \sum_\mu e^{-i\mu\phi_b} \cdot \sum_{\lambda=|\mu|}^{\infty} (X_\mu^\lambda(E) + X_\mu^\lambda(M) + X_\mu^\lambda(G)) K_\mu \left(\frac{|\omega|b}{\gamma v} \right). \quad (4.12)$$

$X_\mu^\lambda(E)$ and $X_\mu^\lambda(M)$ in equation (4.12) are the same as in equations (4.11a and 4.11b), but $X_\mu^\lambda(G)$ is defined by

$$X_\mu^\lambda(G) \equiv \left(1 - \frac{\omega_{\gamma\alpha}}{\omega}\right) \frac{\mathcal{G}_{\lambda\mu}}{i\omega_{\gamma\alpha}} \int d^3r [\mathbf{J}_T(\mathbf{r})]_{\gamma\alpha} \cdot \nabla j_\lambda \left(\frac{|\omega|}{c} r \right) Y_\mu^\lambda(\hat{\mathbf{r}}). \quad (4.13)$$

4.5 Monopole matrix elements

Inspection of equation (4.10) and (4.11a, 4.11b and 4.11c) shows that $[V_{\text{eff}}^{\text{F.T.}}(\omega)]_{\gamma\alpha}$ can be expressed as

$$[V_{\text{eff}}^{\text{F.T.}}(\omega)]_{\gamma\alpha} = \int d^3r [\mathbf{J}_{\text{T}}(\mathbf{r})]_{\gamma\alpha} \cdot \mathbf{Q}_{\text{eff}}(\mathbf{r}) \quad (4.14)$$

where $\mathbf{Q}_{\text{eff}}(\mathbf{r})$ is a linear combination of $(\nabla \times \mathbf{L})j_\lambda(\frac{\omega}{c}r)Y_\mu^\lambda(\hat{\mathbf{r}})$, $\mathbf{L}j_\lambda(\frac{\omega}{c}r)Y_\mu^\lambda(\hat{\mathbf{r}})$, and $\nabla r^\lambda Y_\mu^\lambda(\hat{\mathbf{r}})$. Since

$$\nabla \cdot (\nabla \times \mathbf{L})j_\lambda(\frac{\omega}{c}r)Y_\mu^\lambda(\hat{\mathbf{r}}) = 0, \quad \nabla \cdot \mathbf{L}j_\lambda(\frac{\omega}{c}r)Y_\mu^\lambda(\hat{\mathbf{r}}) = 0, \quad \nabla \cdot \nabla r^\lambda Y_\mu^\lambda(\hat{\mathbf{r}}) = 0,$$

it follows that

$$\nabla \cdot \mathbf{Q}_{\text{eff}}(\mathbf{r}) = 0. \quad (4.15)$$

Now suppose that ϕ_α and ϕ_γ are both states of total angular momentum zero ($J = 0$). Then $[\mathbf{J}_{\text{T}}(\mathbf{r})]_{\gamma\alpha}$ is a spherically-symmetric vector field (a *central* field), and can be written as the gradient of a spherically-symmetric scalar field:

$$[\mathbf{J}_{\text{T}}(\mathbf{r})]_{\gamma\alpha} = \nabla\psi(r).$$

Equations (4.14) and (4.15) imply that

$$[V_{\text{eff}}^{\text{F.T.}}(\omega)]_{\gamma\alpha} = \int d^3r \nabla\psi(r) \cdot \mathbf{Q}_{\text{eff}}(\mathbf{r}) = - \int d^3r \psi(r) \nabla \cdot \mathbf{Q}_{\text{eff}}(\mathbf{r}) = 0.$$

so that the matrix elements of V_{eff} between any two $J = 0$ states vanish identically. Thus an excited $J = 0$ state, in a nucleus with a $J = 0$ ground state, can only be populated indirectly, via a multi-step process. However, if $[V_{\text{cl}}^{\text{F.T.}}(\omega)]_{\gamma\alpha}$ is expressed as

$$[V_{\text{cl}}^{\text{F.T.}}(\omega)]_{\gamma\alpha} = \int d^3r [\mathbf{J}_{\text{T}}(\mathbf{r})]_{\gamma\alpha} \cdot \mathbf{Q}_{\text{cl}}(\mathbf{r}), \quad (4.16)$$

then one of the components in the expansion of $\mathbf{Q}_{\text{cl}}(\mathbf{r})$ is $\nabla j_\lambda(|\omega|r/c)Y_\mu^\lambda(\hat{\mathbf{r}})$ (see equations (4.12,4.13). But

$$\nabla \cdot \nabla j_\lambda \left(\frac{|\omega|}{c}r \right) Y_\mu^\lambda(\hat{\mathbf{r}}) = \nabla^2 j_\lambda \left(\frac{|\omega|}{c}r \right) Y_\mu^\lambda(\hat{\mathbf{r}}) = - \left(\frac{\omega}{c} \right)^2 j_\lambda \left(\frac{|\omega|}{c}r \right) Y_\mu^\lambda(\hat{\mathbf{r}}),$$

which is not identically zero. Thus $\nabla \cdot \mathbf{Q}_{\text{cl}}(\mathbf{r})$ is not identically zero and there is no reason to expect matrix elements of V_{cl} between $J = 0$ states to vanish. A calculation based on V_{cl} implies the possibility of one-step population of an excited $J = 0$ state from a $J = 0$ ground state.

5 Numerical comparisons of V_{eff} and V_{cl}

The following numerical comparisons refer to Coulomb excitation of the giant dipole resonance (GDR) in a ^{40}Ca target by a ^{208}Pb projectile. The target transition current density matrix elements $[\mathbf{J}_T(\mathbf{r})]_{\gamma\alpha}$ needed in equations (3.20) and (4.5) are calculated using Brink's model [18] of the GDR, in which unexcited proton and neutron spheres undergo harmonic oscillations relative to each other. The radial densities of the spheres are obtained by filling the lowest available shell-model single-particle states. The relative harmonic oscillations of the proton and neutrons spheres are characterized by the eigenstates $\phi_m^{n,\ell}(\mathbf{r}_{\text{pn}})$ of a three-dimensional harmonic oscillator. The ground state is $\phi_0^{0,0}$. The degenerate first excited states that can be populated by Coulomb excitation are $\phi_0^{0,1}$ and $(\phi_1^{0,1} + \phi_{-1}^{0,1})/\sqrt{2}$, the combination of $\phi_{\pm 1}^{0,1}$ symmetric under reflection across the reaction plane. In Figure 2, $\mu = 0$ refers to the transition $\phi_0^{0,0} \rightarrow \phi_0^{0,1}$ and $\mu = 1$ refers to the transition $\phi_0^{0,0} \rightarrow (\phi_1^{0,1} + \phi_{-1}^{0,1})/\sqrt{2}$. In every case, the solid line gives $V_{\text{eff}}^{\text{F.T.}}(\omega)$, whereas the dashed line gives $V_{\text{cl}}^{\text{F.T.}}(\omega)$.

In the calculations represented in Figure 2, it has been assumed that the 82 protons of ^{208}Pb are distributed uniformly within a sphere of radius 7.5 fm (as seen by an observer moving with the projectile). The parameters used for the calculations imply that $b = 20$ fm and $\omega_{\gamma\alpha} = 11.7$ MeV/ \hbar . It can be verified by inspection of Figure 2 that, in every case, $V_{\text{eff}}^{\text{F.T.}}$ and $V_{\text{cl}}^{\text{F.T.}}$ agree at $\omega = 11.7$ MeV/ \hbar , as required by equation (4.6).

The first observation concerning Figure 2 is that at a bombarding energy of $E/A=100$ MeV, there is little difference between V_{eff} and V_{cl} . However, at $E/A=10$ GeV, the difference is pronounced. The most striking difference is the very strong increase with bombarding energy of V_{cl} for the $\mu = 0$ transition. This is an expression of the logarithmic divergence (with increasing γ) of the $\mu = 0$ matrix elements of V_{cl} , as shown in equation (4.7). It is clear that, at high bombarding energy, calculations using V_{cl} will ascribe a much higher role to $\mu = 0$ transitions than will calculations using V_{eff} .

Figure 2 also shows that, at high bombarding energy, the photon-exchange mechanism leads to an interaction that is more adiabatic than predicted by the classical electromagnetic field. The wider spread of $V_{\text{cl}}^{\text{F.T.}}(\omega)$, as a function of ω , compared to the spread of $V_{\text{eff}}^{\text{F.T.}}(\omega)$, shows that the impulse provided by the highly-retarded classical field is sharper than the photon-exchange impulse. For example, Figure 3 shows the same comparison as in the $E/A = 10$ GeV, $\mu = 1$ plot of Figure 2, but in the time domain. The sharpness of the pulse provided by $V_{\text{cl}}(t)$, compared with that provided by $V_{\text{eff}}(t)$, is evident. Note that in this particular case, $[V_{\text{cl}}^{\text{F.T.}}(-\omega)]_{\gamma\alpha} = [V_{\text{cl}}^{\text{F.T.}}(\omega)]_{\gamma\alpha}$ which has the consequence that $[V_{\text{cl}}(t)]_{\gamma\alpha}$ is real. However, this is not true of $[V_{\text{eff}}^{\text{F.T.}}(\omega)]_{\gamma\alpha}$, and thus $[V_{\text{eff}}(t)]_{\gamma\alpha}$ has both real and imaginary parts.

6 Comparison of the effects of V_{eff} and V_{cl} in coupled-channel calculations.

The most significant test of the differences between V_{eff} and V_{cl} is in the calculation of RCE cross-sections, since the cross-section is the point where theory and experiment intersect. In this Section, we compare cross-sections calculated with these two interactions, for the $^{208}\text{Pb} +$

^{40}Ca system described in Section 5. We have performed coupled-channel time-integrations of the set of equations (2.6a). The target states included in the calculation span the 0-phonon, 1-phonon, and 2-phonon states of the ^{40}Ca GDR. The methods used to do the numerical Fourier transform needed in equation (3.18b), and to integrate the coupled equations, are described in Reference [12]. We also describe there the integrations over impact parameter needed to calculate the cross-section.

Figure 4 compares the calculated cross-sections for the population of the six reflection-symmetric 1- and 2-phonon states that can be reached via RCE, as functions of the kinetic energy of the ^{208}Pb projectile nucleus. In every case, a solid line is used to show the result of the calculation using $V_{\text{eff}}(t)$, and a dashed line is used to show the result of the corresponding calculation using $V_{\text{cl}}(t)$.

For the one-phonon states, the situation is similar to that shown in Figure 2. The two sets of calculations agree at low bombarding energy ($E/A \lesssim 1$ GeV). However, at high bombarding energy ($E/A \gtrsim 5$ GeV), $V_{\text{cl}}(t)$ predicts much greater cross-sections for the population of the $J = 1, M = 0$ state than does $V_{\text{eff}}(t)$. The situation is more complicated for the two-phonon states. The cross-sections are much smaller than for the one-phonon states, and depend upon multiple excitation processes. Also, the truncation of our calculation at two phonons introduces an additional element of uncertainty into our two-phonon cross-sections. However, it is noteworthy that the 2-phonon $|M| = 1$ state is also strongly favored by $V_{\text{cl}}(t)$ at high bombarding energy, compared to $V_{\text{eff}}(t)$. The reason is that this state is mostly populated in two-step processes, such as

$$(J = M = 0) \rightarrow (J = 1, M = 0) \rightarrow (J = 2, |M| = 1)$$

and

$$(J = M = 0) \rightarrow (J = 1, |M| = 1) \rightarrow (J = 2, |M| = 1).$$

In both cases, a $\Delta M = 0$ transition is involved, and it is the logarithmic divergence (with increasing γ) of the $\Delta M = 0$ transition amplitude that leads to the strongly increasing cross-section when $V_{\text{cl}}(t)$ is used. But the $J = 2, |M| = 2$ state is reached mainly by

$$(J = M = 0) \rightarrow (J = 1, |M| = 1) \rightarrow (J = 2, |M| = 2),$$

in which there is no $\Delta M = 0$ step, and so the $J = 2, |M| = 2$ state is not strongly favored by $V_{\text{cl}}(t)$ at high bombarding energy. Thus we see that for $E/A \gtrsim 5$ GeV, $V_{\text{eff}}(t)$ and $V_{\text{cl}}(t)$ predict very different cross-sections when used in coupled-channel analyses. A calculation using $V_{\text{cl}}(t)$ will predict strongly enhanced cross-sections for populating any state that can be reached via a one-step or two-step process involving a $\Delta M = 0$ transition.

The expression for $V_{\text{cl}}^{\text{F.T.}}(\omega)$ given by equation (4.5) depends upon the total projectile charge, but not on the radial dependence of this charge. However there *is* a dependence on the projectile radial charge density in $V_{\text{eff}}^{\text{F.T.}}(\omega)$ given by equation (3.20). Fortunately, this dependence is very weak. The calculations using $V_{\text{eff}}^{\text{F.T.}}(\omega)$ whose results are shown in Figure 4, were done using a radial charge distribution which was constant from the center out to 7.5 fm. By way of comparison, we have repeated these calculations, assuming that all the charge of the ^{208}Pb nucleus is concentrated at its center. In all cases, we found that the calculated cross-sections

changed by no more than a few tenths of a percent. As might be expected, the transition amplitudes are more sensitive to projectile radial density at small impact parameters. However, when the integration over all impact parameters is done, the residual effect on the cross-section of changes in the projectile radial charge density is very small.

7 Conclusions and discussion.

We have been concerned with a situation in which a target nucleus experiences the effects of a time-dependent electromagnetic field produced by a rapidly moving projectile. We have shown that if this is assumed to be the *classical* electromagnetic field of the projectile, serious problems arise, such as a $\log \gamma$ divergence of $\Delta M = 0$ transitions at large γ . These problems are not present if the quantum nature of the electromagnetic field is taken into account. We have shown that this can be done within the framework of the time-dependent coupled-channel approach to RCE, by means of an interaction potential $V_{\text{eff}}(t)$, which includes the effects of photon exchange between the projectile and target. We have presented an explicit expression for $V_{\text{eff}}(t)$, and derived its multipole expansion. Since it is free of the large- γ divergence, we believe that $V_{\text{eff}}(t)$ should be used in time-dependent RCE calculations, instead of $V_{\text{cl}}(t)$, whenever the bombarding energy per nucleon exceeds approximately 2 GeV.

Although $V_{\text{eff}}(t)$ and $V_{\text{cl}}(t)$ can give quite different results for time-dependent calculations, their Fourier transforms are equal at onshell frequencies. Therefore $V_{\text{cl}}(t)$ and $V_{\text{eff}}(t)$ can be used interchangeably in any calculation that does not go beyond first-order perturbation theory. Calculations which use the FWW “method of virtual quanta” [16] are of this type. They are based on the *classical* fields produced by the potential which, at large γ , can be approximated by the fields of a plane electromagnetic wave. The virtual photons have momenta parallel to the projectile direction, and simulate the effects of the plane wave. Note that these photons can only induce target $\Delta M = \pm 1$ transitions. There are also classical *longitudinal* fields, but their effects are smaller by a factor of $\sim 1/\gamma^2$. This is precisely the situation with onshell $\Delta M = 0$ matrix elements, which are suppressed relative to offshell $\Delta M = 0$ matrix elements by a factor of $\sim 1/\gamma^2$. Thus the FWW method can be regarded as a description of high-energy first-order perturbation theory. The strong off-shell $\Delta M = 0$ matrix elements of $V_{\text{cl}}(t)$ are not present in the FWW method, which emphasizes that FWW describes only *onshell* aspects of the interaction.

It is important to emphasize that the virtual photons of the FWW method are quite different from the photons whose exchange between projectile and target were described in Section 3. Those photons were excitations of the quantum states of the electromagnetic field, which is a real part of our physical system. The FWW photons are a convenient way of describing a classical electromagnetic field, that is itself a convenient way of presenting a first-order perturbation treatment of the interaction. Moreover, it is clear that *no* photon that can be coupled to the vacuum by the $(-1/c)\mathbf{J}_P \cdot \mathbf{A}$ interaction can have its momentum parallel to the projectile trajectory. However *all* of the FWW virtual photons have momenta parallel to the projectile trajectory.

APPENDICES

A Intermediate steps in the derivation of equation (3.16)

The \mathbf{r} integrals in equation (3.10) can be performed with the aid of equations (3.14b and 3.15). The result is

$$\int e^{-i\mathbf{q}\cdot\hat{\mathbf{e}}_{\mathbf{q},j}^*\cdot\mathbf{J}_P(\mathbf{r},t'')}d^3r = 4\pi v\hat{\mathbf{e}}_{\mathbf{q},j}^* \int_0^\infty \tilde{r}^2 d\tilde{r} \tilde{\rho}_P(\tilde{r}) j_0\left(\tilde{r}\sqrt{q_\perp^2 + \left(\frac{q_z}{\gamma}\right)^2}\right) e^{-i\mathbf{q}_\perp\cdot\mathbf{b}-iq_z vt''}$$

and the β_1 sum in equation (3.7) is

$$P_1(t) \equiv \frac{v}{i\pi^2} \int \frac{d^3q}{q} \int_0^\infty \tilde{r}^2 d\tilde{r} \tilde{\rho}_P(\tilde{r}) j_0\left(\tilde{r}\sqrt{q_\perp^2 + \left(\frac{q_z}{\gamma}\right)^2}\right) \times \int d^3r \sum_j \hat{\mathbf{e}}_{\mathbf{q},j}^* \cdot \hat{\mathbf{z}} \hat{\mathbf{e}}_{\mathbf{q},j} \cdot [\mathbf{J}_T(\mathbf{r})]_{\gamma\alpha} e^{i\mathbf{q}\cdot(\mathbf{r}-\mathbf{b})} \int_{-\infty}^{t'} e^{i[cq(t''-t')-q_z vt'']} dt'' \quad (\text{A.1})$$

To make the t'' integration meaningful, we use the familiar adiabatic switching-on procedure [15]:

$$\begin{aligned} \int_{-\infty}^{t'} e^{i(cq-q_z v)t''} dt'' &\equiv \lim_{\eta\rightarrow 0^+} \int_{-\infty}^{t'} e^{[i(cq-q_z v)+\eta]t''} dt'' = \lim_{\eta\rightarrow 0^+} \frac{e^{[i(cq-q_z v)+\eta]t'}}{i(cq-q_z v)+\eta} \Big|_{-\infty}^{t'} \\ &= \frac{e^{i(cq-q_z v)t'}}{i(cq-q_z v)}, \end{aligned}$$

which leads to

$$P_1(t) = -\frac{v}{\pi c} \int \frac{d^3q}{q(cq-q_z v)} e^{-iq_z vt'} \int_0^\infty \tilde{r}^2 d\tilde{r} \tilde{\rho}_P(\tilde{r}) j_0\left(\tilde{r}\sqrt{q_\perp^2 + \left(\frac{q_z}{\gamma}\right)^2}\right) \times \int d^3r \sum_j \hat{\mathbf{e}}_{\mathbf{q},j}^* \cdot \hat{\mathbf{z}} \hat{\mathbf{e}}_{\mathbf{q},j} \cdot [\mathbf{J}_T(\mathbf{r})]_{\gamma\alpha} e^{i\mathbf{q}_\perp\cdot(\mathbf{r}-\mathbf{b})} \quad (\text{A.2})$$

The j -sum can be performed by noting that $(\hat{\mathbf{q}}, \hat{\mathbf{e}}_{\mathbf{q},1}, \hat{\mathbf{e}}_{\mathbf{q},2})$ form a complete orthonormal set of vectors. Thus

$$[\mathbf{J}_T]_z \equiv \mathbf{J}_T \cdot \hat{\mathbf{z}} = (\mathbf{J}_T \cdot \hat{\mathbf{q}})(\hat{\mathbf{z}} \cdot \hat{\mathbf{q}}) + (\mathbf{J}_T \cdot \hat{\mathbf{e}}_{\mathbf{q},1})(\hat{\mathbf{z}} \cdot \hat{\mathbf{e}}_{\mathbf{q},1}) + (\mathbf{J}_T \cdot \hat{\mathbf{e}}_{\mathbf{q},2})(\hat{\mathbf{z}} \cdot \hat{\mathbf{e}}_{\mathbf{q},2}),$$

so that

$$\sum_{j=1,2} (\mathbf{J}_T \cdot \hat{\mathbf{e}}_{\mathbf{q},j})(\hat{\mathbf{z}} \cdot \hat{\mathbf{e}}_{\mathbf{q},j}^*) = [\mathbf{J}_T]_z - (\mathbf{J}_T \cdot \hat{\mathbf{q}})(\hat{\mathbf{z}} \cdot \hat{\mathbf{q}}) = [\mathbf{J}_T]_z - \frac{(\mathbf{J}_T \cdot \mathbf{q})q_z}{q^2},$$

and equation (A.2) becomes

$$\begin{aligned} \sum_{\beta_1} &= -\frac{v}{\pi c} \int \frac{d^3 q}{q(cq - q_z v)} e^{-iq_z vt'} \int_0^\infty \tilde{r}^2 d\tilde{r} \tilde{\rho}_P(\tilde{r}) j_0 \left(\tilde{r} \sqrt{q_\perp^2 + \left(\frac{q_z}{\gamma}\right)^2} \right) \\ &\times \int d^3 r \left[[\mathbf{J}_T]_z - \frac{(\mathbf{J}_T \cdot \mathbf{q}) q_z}{q^2} \right]_{\gamma\alpha} e^{i\mathbf{q}_\perp \cdot (\mathbf{r} - \mathbf{b})} \end{aligned} \quad (\text{A.3a})$$

The β_2 sum in equation (3.7) is performed in exactly the same way, except that (3.9b) is used, and the t'' integral is replaced by

$$\int_{t'}^\infty dt'' e^{i(q_z v - cq)t''} \equiv \lim_{\eta \rightarrow 0_+} \int_{t'}^\infty dt'' e^{[i(q_z v - cq) - \eta]t''} = \frac{e^{i(q_z v - cq)t'}}{i(q_z v - cq)}.$$

The result is

$$\begin{aligned} P_2(t) &= -\frac{v}{\pi c} \int \frac{d^3 q}{q(cq + q_z v)} e^{-iq_z vt'} \int_0^\infty \tilde{r}^2 d\tilde{r} \tilde{\rho}_P(\tilde{r}) j_0 \left(\tilde{r} \sqrt{q_\perp^2 + \left(\frac{q_z}{\gamma}\right)^2} \right) \\ &\times \int d^3 r \left[[\mathbf{J}_T]_z - \frac{(\mathbf{J}_T \cdot \mathbf{q}) q_z}{q^2} \right]_{\gamma\alpha} e^{i\mathbf{q}_\perp \cdot (\mathbf{r} - \mathbf{b})} \end{aligned} \quad (\text{A.3b})$$

We add $P_1(t)$ from equation (A.3a) to $P_2(t)$ from equation (A.3b) to get the total photon-exchange contribution, $P(t)$. Using

$$\frac{1}{cq - q_z v} + \frac{1}{cq + q_z v} = \frac{2cq}{(cq)^2 - (q_z v)^2} = \frac{2q}{c} \frac{1}{q_\perp^2 + q_z^2 - \frac{v^2}{c^2} q_z^2} = \frac{2q}{c} \frac{1}{q_\perp^2 + \left(\frac{q_z}{\gamma}\right)^2},$$

we obtain the result given in equation (3.16).

B Two integral relations

Define $I(\tilde{r})$ by

$$I(\tilde{r}) \equiv \int \frac{d^2 \mathbf{q}_\perp}{q_\perp^2 + \lambda_1^2} e^{i\mathbf{q}_\perp \cdot (\boldsymbol{\rho} - \mathbf{b})} j_0 \left(\tilde{r} \sqrt{q_\perp^2 + \lambda_2^2} \right). \quad (\text{B.1})$$

Operate on this expression with $\nabla_{\tilde{\mathbf{r}}}^2$:

$$\begin{aligned}
\nabla_{\tilde{\mathbf{r}}}^2 I(\tilde{r}) &= \int \frac{d^2 \mathbf{q}_\perp}{q_\perp^2 + \lambda_1^2} e^{i\mathbf{q}_\perp \cdot (\boldsymbol{\rho} - \mathbf{b})} \nabla_{\tilde{\mathbf{r}}}^2 j_0 \left(\tilde{r} \sqrt{q_\perp^2 + \lambda_2^2} \right) \\
&= - \int d^2 \mathbf{q}_\perp \frac{q_\perp^2 + \lambda_2^2}{q_\perp^2 + \lambda_1^2} e^{i\mathbf{q}_\perp \cdot (\boldsymbol{\rho} - \mathbf{b})} j_0 \left(\tilde{r} \sqrt{q_\perp^2 + \lambda_2^2} \right) \\
&= - \int d^2 \mathbf{q}_\perp \left(1 + \frac{\lambda_2^2 - \lambda_1^2}{q_\perp^2 + \lambda_1^2} \right) e^{i\mathbf{q}_\perp \cdot (\boldsymbol{\rho} - \mathbf{b})} j_0 \left(\tilde{r} \sqrt{q_\perp^2 + \lambda_2^2} \right) \\
&= - \int d^2 \mathbf{q}_\perp e^{i\mathbf{q}_\perp \cdot (\boldsymbol{\rho} - \mathbf{b})} j_0 \left(\tilde{r} \sqrt{q_\perp^2 + \lambda_2^2} \right) \\
&\quad - (\lambda_2^2 - \lambda_1^2) \int \frac{d^2 \mathbf{q}_\perp}{q_\perp^2 + \lambda_1^2} e^{i\mathbf{q}_\perp \cdot (\boldsymbol{\rho} - \mathbf{b})} j_0 \left(\tilde{r} \sqrt{q_\perp^2 + \lambda_2^2} \right). \tag{B.2}
\end{aligned}$$

In the first term of equation (B.2), replace $j_0 \left(\tilde{r} \sqrt{q_\perp^2 + \lambda_2^2} \right)$ by

$$j_0 \left(\tilde{r} \sqrt{q_\perp^2 + \lambda_2^2} \right) = \frac{1}{4\pi} \int \sin \tilde{\theta} d\tilde{\theta} d\tilde{\phi} e^{-i(\mathbf{q}_\perp \cdot \tilde{\boldsymbol{\rho}} + \lambda_2 \tilde{z})}$$

where $\tilde{\boldsymbol{\rho}} \equiv \tilde{r} \sin \tilde{\theta} (\cos \tilde{\phi} \hat{\mathbf{x}} + \sin \tilde{\phi} \hat{\mathbf{y}})$ and $\tilde{z} = \tilde{r} \cos \tilde{\theta}$. Then equation (B.2) becomes

$$\begin{aligned}
\nabla_{\tilde{\mathbf{r}}}^2 I(\tilde{r}) &= -\frac{1}{4\pi} \int \sin \tilde{\theta} d\tilde{\theta} d\tilde{\phi} \int d^2 \mathbf{q}_\perp e^{i\mathbf{q}_\perp \cdot (\boldsymbol{\rho} - \mathbf{b} - \tilde{\boldsymbol{\rho}})} e^{-i\lambda_2 \tilde{z}} \\
&\quad - (\lambda_2^2 - \lambda_1^2) \int \frac{d^2 \mathbf{q}_\perp}{q_\perp^2 + \lambda_1^2} e^{i\mathbf{q}_\perp \cdot (\boldsymbol{\rho} - \mathbf{b})} j_0 \left(\tilde{r} \sqrt{q_\perp^2 + \lambda_2^2} \right) \\
\nabla_{\tilde{\mathbf{r}}}^2 I(\tilde{r}) + (\lambda_2^2 - \lambda_1^2) I(\tilde{r}) &= -\frac{(2\pi)^2}{4\pi} \int \sin \tilde{\theta} d\tilde{\theta} d\tilde{\phi} e^{-i\lambda_2 \tilde{z}} \delta(\boldsymbol{\rho} - \mathbf{b} - \tilde{\boldsymbol{\rho}}). \tag{B.3}
\end{aligned}$$

In our application, $|\boldsymbol{\rho}|$ is bounded by the radius of the target and $|\tilde{\boldsymbol{\rho}}|$ is bounded by the radius of the projectile. The condition that the projectile and target do not overlap implies that $|\boldsymbol{\rho} - \mathbf{b}| > |\tilde{\boldsymbol{\rho}}|$ for every orientation $\tilde{\theta}, \tilde{\phi}$, and so $\boldsymbol{\rho} - \mathbf{b} - \tilde{\boldsymbol{\rho}}$ is never zero. Thus the δ -function on the right-hand side of equation (B.3) vanishes, and we get

$$\nabla_{\tilde{\mathbf{r}}}^2 I(\tilde{r}) + (\lambda_2^2 - \lambda_1^2) I(\tilde{r}) = 0. \tag{B.4}$$

We have two applications of equation (B.4). In one of them, $\lambda_1^2 = \lambda_2^2 = (\omega/(\gamma v))^2$. In the other, $\lambda_1^2 = (\omega/v)^2$, $\lambda_2^2 = (\omega/(\gamma v))^2$. Thus in both cases, $(\lambda_2^2 - \lambda_1^2) \leq 0$, and we can write the general solution of equation (B.4) as

$$I(\tilde{r}) = \alpha j_0 \left(i\tilde{r} \sqrt{\lambda_1^2 - \lambda_2^2} \right) + \beta n_0 \left(i\tilde{r} \sqrt{\lambda_1^2 - \lambda_2^2} \right), \tag{B.5}$$

where α and β are independent of \tilde{r} . The first term in equation (B.5) is finite at $\tilde{r} = 0$, whereas the second term diverges there. But if we set $\tilde{r} = 0$ in the definition (B.1), we get

$$I(0) = \int \frac{d^2 \mathbf{q}_\perp}{q_\perp^2 + \lambda_1^2} e^{i\mathbf{q}_\perp \cdot (\boldsymbol{\rho} - \mathbf{b})} = 2\pi K_0(|\lambda_1| |\boldsymbol{\rho} - \mathbf{b}|) \tag{B.6}$$

which is finite in our $|\boldsymbol{\rho} - \mathbf{b}| \geq 0$ situation. Thus β in equation (B.5) vanishes and

$$I(0) = \alpha j_0(0) = \alpha = 2\pi K_0(|\lambda_1| |\boldsymbol{\rho} - \mathbf{b}|),$$

leading to

$$I(\tilde{r}) \equiv \int \frac{d^2 \mathbf{q}_\perp}{q_\perp^2 + \lambda_1^2} e^{i \mathbf{q}_\perp \cdot (\boldsymbol{\rho} - \mathbf{b})} j_0 \left(\tilde{r} \sqrt{q_\perp^2 + \lambda_2^2} \right) = 2\pi K_0(|\lambda_1| |\boldsymbol{\rho} - \mathbf{b}|) j_0 \left(i \tilde{r} \sqrt{\lambda_1^2 - \lambda_2^2} \right). \quad (\text{B.7})$$

Thus we get the two special cases:

$$\int \frac{d^2 \mathbf{q}_\perp}{q_\perp^2 + \left(\frac{\omega}{\gamma v}\right)^2} e^{i \mathbf{q}_\perp \cdot (\boldsymbol{\rho} - \mathbf{b})} j_0 \left(\tilde{r} \sqrt{q_\perp^2 + \left(\frac{\omega}{\gamma v}\right)^2} \right) = 2\pi K_0 \left(\frac{|\omega| |\boldsymbol{\rho} - \mathbf{b}|}{\gamma v} \right) \quad (\text{B.8a})$$

$$\int \frac{d^2 \mathbf{q}_\perp}{q_\perp^2 + \left(\frac{\omega}{v}\right)^2} e^{i \mathbf{q}_\perp \cdot (\boldsymbol{\rho} - \mathbf{b})} j_0 \left(\tilde{r} \sqrt{q_\perp^2 + \left(\frac{\omega}{v}\right)^2} \right) = 2\pi K_0 \left(\frac{|\omega| |\boldsymbol{\rho} - \mathbf{b}|}{v} \right) j_0 \left(i \tilde{r} \frac{|\omega|}{c} \right). \quad (\text{B.8b})$$

These equations are valid when $\tilde{r} < |\boldsymbol{\rho} - \mathbf{b}|$.

References

- [1] A. Winther and K. Alder, Nucl. Phys. **A319**, 518 (1979).
- [2] D. Galetti, T. Kodama, and M.C. Nemes, Annals of Physics **177**, 229 (1987)
- [3] C.A. Bertulani, A.E. Stuchbery, T.J. Mertzimekis, and A.D. Davies, Phys. Rev. C **68**, 044609 (2003)
- [4] K. Alder, A. Bohr, T. Huus, B. Mottelson, and A. Winther, Rev. Mod. Phys. **28**, 432 (1956)
- [5] C.A. Bertulani and G. Baur, Phys. Rep. **163**, 299 (1988).
- [6] H. Emling, Progr. Part. Nucl. Phys. **33**, 729 (1994).
- [7] Ph. Chomaz and N. Francaria, Phys. Rep. **252**, 275 (1995).
- [8] C.A. Bertulani, L.F. Canto, M.S. Hussein, and A.F.R. de Toledo Piza, Phys. Rev. C **53**, 334 (1996).
- [9] E.G. Lanza, M.V. Andres, F. Catara, Ph. Chomaz, and C. Volpe, Nucl. Phys. **A613**, 445 (1997).
- [10] T. Aumann, P.F. Bortignon, and H. Emling, Annu. Rev. Nucl. Part. Sci. **48**, 351 (1998).
- [11] B.F. Bayman and F. Zardi, Phys. Rev. C **59**, 2189 (1999).
- [12] B.F. Bayman and F. Zardi, Phys. Rev. C **68** 014905 (2003).

- [13] C.A. Bertulani and V.Yu. Ponomarev, Phys. Rep. **321**, 139 (1999).
- [14] W. Heitler, *The Quantum Theory of Radiation* (Clarendon Press, Oxford, 1954).
- [15] J.J. Sakurai, *Advanced Quantum Mechanics* (Addison-Wesley Publishing Co., Reading, Mass, 1967).
- [16] J.D. Jackson, *Classical Electrodynamics* (John Wiley & Sons, New York, 1975).
- [17] L.C. Biedenharn, J.L. McHale, and R.M. Thaler, Phys. Rev. **100**, 376 (1955).
- [18] D. M. Brink, Nucl. Phys. **4**, 215 (1957)

Figure Captions

Figure 1. (a) The intermediate state β_1 consists of the target in its initial state plus a \mathbf{q}, j photon. (b) The intermediate state β_2 consists of the target in its final state plus a \mathbf{q}, j photon.

Figure 2. Plots of matrix elements of $V^{\text{F.T.}}(\omega)$ connecting the ^{40}Ca ground state to the one-phonon giant dipole resonance states. The projectile is a ^{208}Pb nucleus with bombarding energy per nucleon E/A . $\mu = 0$ corresponds to the $M = 0$ one-phonon state; $\mu = 1$ to the reflection-symmetric $|M| = 1$ state.

Figure 3. Comparison of $V_{\text{eff}}(t)$ (solid line) and $V_{\text{cl}}(t)$ (dashed line), corresponding to the $E/A = 10$ GeV, $\mu = 1$ example of Figure 2.

Figure 4. Calculated coupled-channel Coulomb excitation cross-sections for one- and two-phonon states of the GDR in ^{40}Ca with ^{208}Pb projectiles. The solid curves correspond to calculations in which the quantized electromagnetic field has been used, the dashed curves to calculations with a classical electromagnetic field.

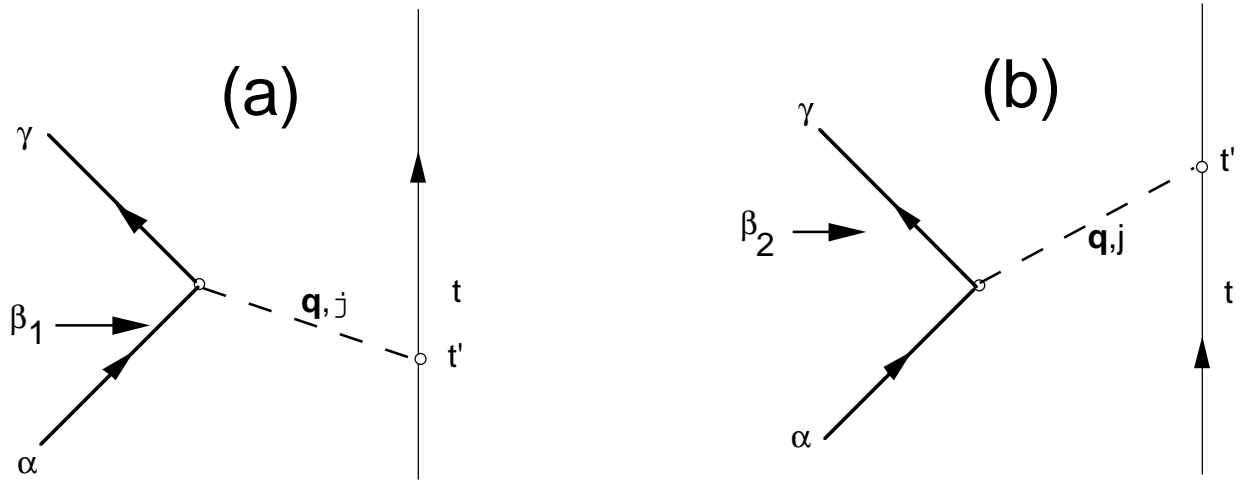


Figure 1. a) β_1 represents the initial state plus a \mathbf{q}, j photon .
 b) β_2 represents the final state plus a \mathbf{q}, j photon .

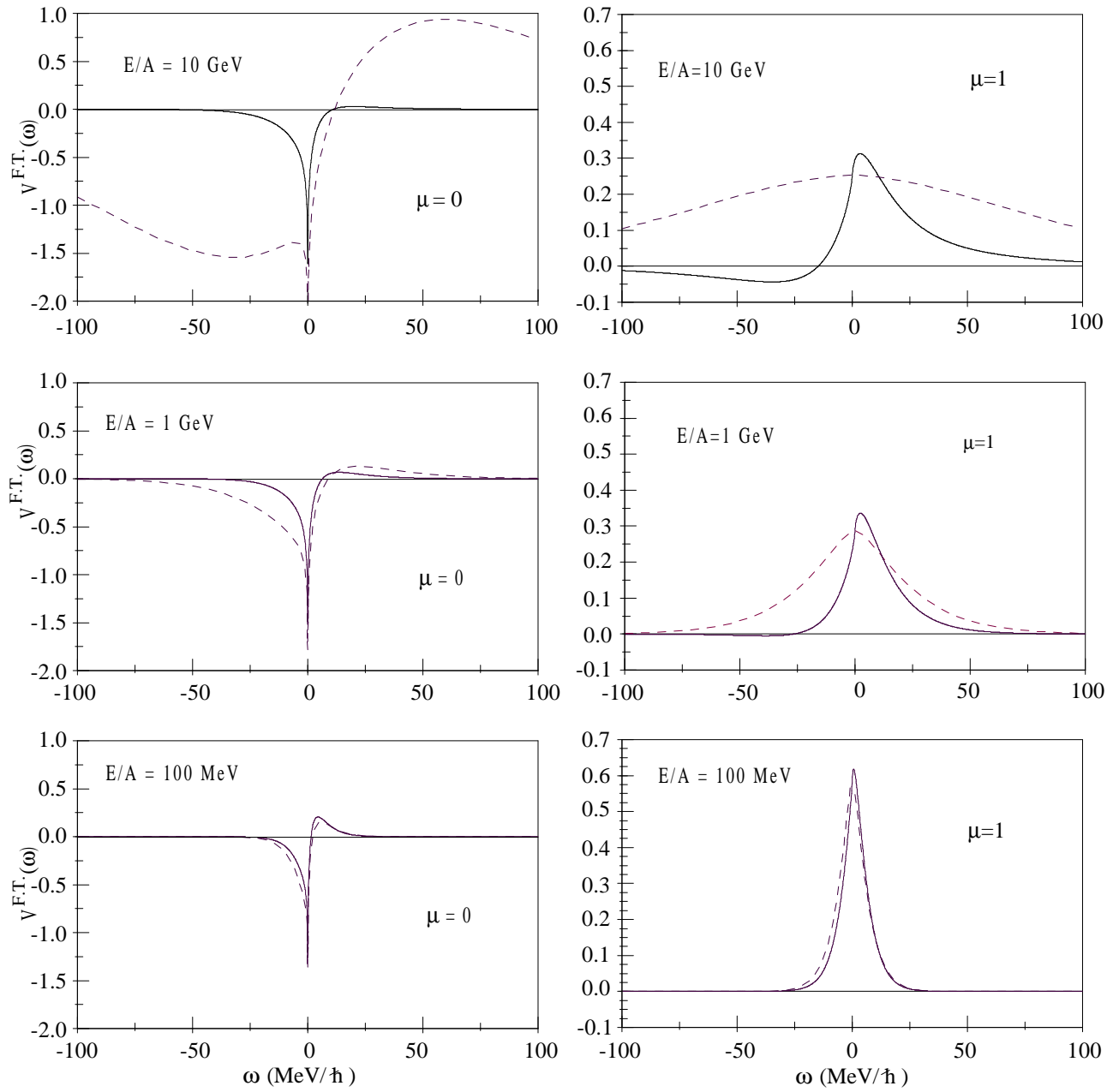


Figure 2. $V^{F.T.}(\omega)$ connecting the ^{40}Ca ground state to 1-phonon GDR states

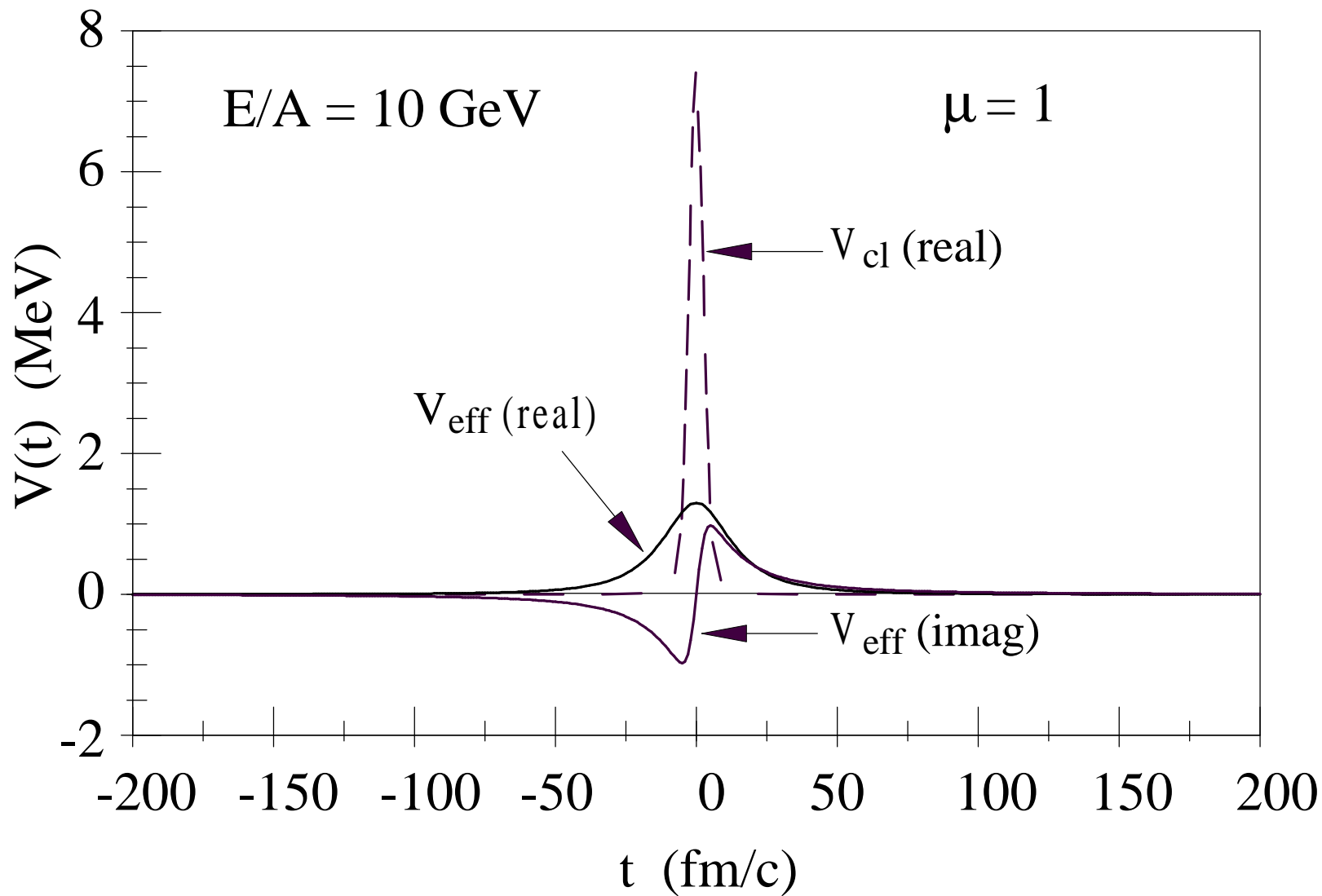


Figure 3. $V(t)$ corresponding to the $E/A=10 \text{ GeV}$, $\mu=1$ case of Figure 2.

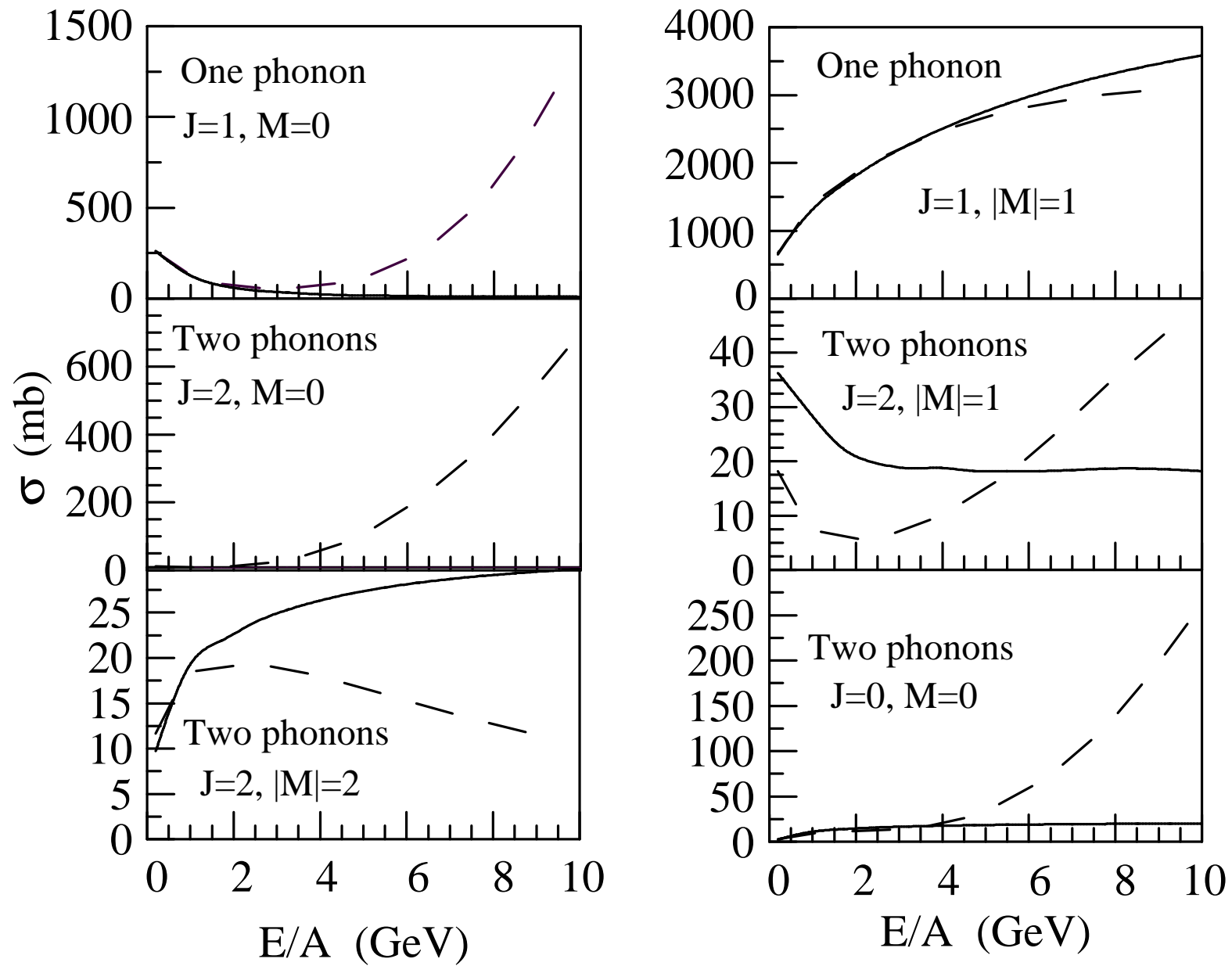


Figure 4. Calculated cross-sections for the 1- & 2-phonon GDR states of ^{40}Ca .